Sudan University of Science and Technology

College of Graduate Studies

Mapping Molecules in Nile Water in Northern Sudan Using Raman Spectroscopy

تخريط الجزيئات في مياه النيل في شمال السودان باستخدام تقنية مطيافية رامان

A Thesis Submitted in Fulfillment of Requirements for the Degree of Ph.D in Laser Applications in Physics

By:

Sufyan Sharafedin Mohammed Dawod

Supervisor:

Professor: Abdelmoneim M. Awadelgied

Co-Supervisor:

Sohad Saad Elwakeel

July 2019

الآية

قال تعالى: (وَاخْفِضْ لَهُمَا جَنَاحَ الذُّلِّ مِنَ الرَّحْمَةِ وَقُل رَّبِّ ارْحَمْهُمَا كَمَا رَبَّيَانِي صَغِيرًا)

صدق الله العظيم

الآية 24 سورة الإسراء

Dedication

A special thanks to my family, Words cannot express how grateful I am to my Mother, the first one who taught me a letter. And my father, from whom I know the meaning of life. To my brother and my sisters the light of my way, for all of the sacrifices that they made on my behalf. I would like also to thank all friends who supported me and incented me to strive towards my goal, especially thanks to Amir Farah and Mohammed Abd El Wahab.

To my dear son, with my sincere love.

Finally I like to express my appreciation to my wife Onab Abd-Elrahman who spent sleepless nights with me and was always my support in the moments when there was no one to answer my queries.

Sufyan

Acknowledgments

First of all praise be to Allah the most merciful, who gave me the ability and strength to complete this work.

I would like to express my sincere gratitude to my supervisor Professor Abdelmoneim M. Awadelgied and the thanks extended to Professor Nafie Abd Allattief Almuslet for the continuous support of my PhD study and related research, for their patience, motivation, and immense knowledge. Their guidance helped me in all the time of research and writing this thesis. I could not have imagined having a better advisor and mentor for my Ph. D study. As well as thanks to Dr. Sohad Saad Elwakeel for the estimated effort.

My sincere thanks also go to Dr. Ali Maarouf, Dean of the Laser Institute, who supports me and helps me in my work. I would also like to thank all the staff at the Laser Institute for their help.

I wish to thank the Indian Institute of Science for recording the Raman spectra.

I would also like to thank Dr. Abd El sakhy Mohammed - Neelain University, Ahmed Abubaker, Mahmoud Mohammed Khairy, Mohammed Ahmed Mahgoub and all the colleagues who supported me in sampling.

Abstract

Spectroscopy is the main field of this research which aims to mapping and characterize the molecules on Nile water in Northern Sudan using Raman spectroscopy. Ten samples of water were collected from different five areas in the northern state (Halfa, Abry, Abu hamd, Atbra and Shendy). Two samples were collected from each area, one from the Nile directly and the other from the water pipeline in sterilized plastic tanks to ensure no water contamination. The samples were tested at the modern Indian Institute using the Horiba Lab RAM HR 3D Raman spectrometer equipped with 532 nm laser source with laser power of 6 mW. Each sample was put in a glass slide of Raman spectrometer and Raman spectra were recorded in wave number range of (0 - 4000 cm - 1). which indicated the existence of molecules (O-H bending, α Fe-OH, Si-O-S, C=S, C-F, ν(C-C) stretching, Toluene, C–H bending, p-xylene, P – H, Lactone, C = C, Si – O – C, NO, Isothiocyanat, Diazonium salt, FeII-O, C–O, $(ASO_4)^{-3}$, Ester, C=O, C≡N stretch, $UO_2{}^{+2}$, C–N–C, $\nu(C-N)_\beta$, NO, Aromatic azo, Amide II, Aromatic nitrile, $CaCO_3$, As–O, Ethylbenzene, Sulfonic acid, FeIII-O, $PO_4{}^{-3}$, C – CH_3, Thiocyanate, S-S, C–H, perchlorate and NO^{-3}).

The results of Raman spectra obtained for samples collected from the five regions were compared with each other. The samples collected from pipeline in Halfa area were found free from toxic molecules such as ($UO_2{}^{+2}$ and P – H) unlike those collected directly from the Nile stream in the same area, whereas, the samples collected from pipeline in Halfa area, the results indicated the existence of ($(ASO_4)^{-3}$, p-xylene and NO) molecules which is strangely enough not observed for Nile stream water.

The samples collected from pipeline in Abry area were found free from other type of toxic molecules such as (C≡N and Toluene) which appeared in samples from

Nile stream in the same area. But concerning in this area, the results indicated the existence of

(C = S, Ethylbenzene and NO) molecules in the pipeline water which were not appeared in Nile stream water.

Also the sample collected from pipeline in Abu Hamad were found free from toxic molecules such as ($ASO_4^{-3}$and PO_4^{-3}) which appeared in sample from Nile stream in the same area. whereas, the sample collected from pipeline in Abu Hamad area, the results indicated the existence of (Toluene, Ethylbenzen and UO_2^{+2}) molecules which is strangely enough not observed for Nile stream water.

The molecules (ASO_4^{-3}, C–N–C, Ethylbenzen and C≡N) were not appeared in the sample collected from pipeline in Atbra area which were found in sample collected from Nile stream water in the same area. But other molecules such as (As–O and $\nu(C-N)_\beta$) were found in the sample collected from pipeline in Atbra area and were not found in sample collected from Nile stream water in the same area.

Finally the sample collected from pipeline in Shandy area were found free from toxic molecules such as ($NO^{-3}$and C≡N) unlike those collected directly from the Nile stream in the same area, whereas, the sample collected from pipeline in Shandy area, the results indicated the existence of (S-S, Aromatic nitrile, $UO_2^{+2}$and $\nu(C-N)_\beta$) molecules which is strangely enough not observed for Nile stream water.

المستخلص

علم الأطياف هو المجال الرئيس لهذا البحث الذي يهدف إلى رصد وتوصيف الجزيئات المكونة لمياه النيل شمال السودان باستخدام تقنية مطيافية رامان. جُمعت عشر عينات من المياه من خمس مناطق مختلفة في الولاية الشمالية (حلفا،عبري، أبوحمد، عطبرة وشندي)، جُمعت عينتين من كل منطقة، واحدة من النيل مباشرة والأخرى من الخط الناقل للمياه في قوارير بلاستيكية معقمة لضمان عدم تلوث المياه. ثم اختبرت العينات في المعهد الهندي الحديث بواسطة جهاز مطيافية الليزر – رامان نوع (Horiba Lab RAM HR 3D) باستخدام مصدر ليزر الثنائي بطول موجي (532 nm) و بقدرة (6 mW). ووُضعت كل عينة من عينات المياه في شريحة زجاجية خاصة بمطيافية رامان وسُجلت أطياف رامان في المدى ($0\text{-}4000cm^{-1}$) لكل العينات والتي تشير إلى وجود جزيئات (O-H bending، α Fe-OH، Si-O-S، C=S، C-F، ν(C-C) stretching، Toluene، C–H bending، p-xylene، P – H، Lactone، C = C، Si – O، C – O، NO، Isothiocyanate، Diazonium salt، FeII-O، C–O، $(ASO_4)^{-3}$ ، Ester، Amide II، Aromatic azo، NO، $\nu(C-N)_\beta$، C–N–C، $UO_2{}^{+2}$، C≡N stretch، C=O، Aromatic nitrile، $CaCO_3$، As–O، Ethylbenzene، FeIII-O، $PO_4{}^{-3}$، C – CH_3 و Thiocyanate).

تمت مقارنة نتائج أطياف رامان المتحصل عليها من العينات التي جمعت من الخمس مناطق. تختلف العينات المجموعة من الخط الناقل للمياه في منطقة حلفا عن العينات المجموعة من مجرى النيل مباشرة في نفس المنطقة بخلوها من بعض الجزيئات السامة مثل ($UO_2{}^{+2}$ و P – H)، بينما وجد أن العينات المجموعة من الخط الناقل للمياه في منطقة حلفا تحتوي على الجزيئات ($(ASO_4)^{-3}$، p-xylene و NO) والتي لم تشاهد في العينات المجموعة من مجرى النيل مباشرة في نفس المنطقة.

وجد أن العينات المجموعة من الخط الناقل للمياه في منطقة عبري خالية من بعض الجزيئات السامة مثل (C≡N و Toluene) والتي ظهرت في العينات المجموعة من مجرى النيل مباشرة لنفس المنطقة. لكن أشارت النتائج أن العينات المجموعة من الخط الناقل للمياه في هذه المنطقة توجد بها جزيئات (C = S، Ethylbenzene و NO) والتي لم تظهر في العينات المجموعة من مجرى النيل في نفس المنطقة.

كما وجد أن العينات المجموعة من الخط الناقل للمياه في منطقة أبو حمد خالية من جزيئات ($ASO_4{}^{-3}$ و $PO_4{}^{-3}$) السامة التي ظهرت في عينات مجري النيل لنفس المنطقة. بينما أشارت النتائج إلى وجود

جزيئات (Toluene، Ethylbenzen و UO_2^{+2}) في العينات المجموعة من الخط الناقل للمياه في منطقة أبو حمد، بغرابة، لم تُشاهد هذه الجزيئات في العينات المجموعة مباشرة من مجرى النيل في نفس المنطقة.

الجزيئات (ASO_4^{-3}، C–N–C، Ethylbenzen و C≡N) لم تظهر في العينات المجموعة من الخط الناقل للمياه في منطقة عطبرة والتي كانت موجودة في العينات المجموعة من مجرى النيل مباشرة في نفس المنطقة. لكن بعض الجزيئات مثل (As–O و $\nu(C-N)_\beta$) وجدت في العينات المجموعة من الخط الناقل للمياه في منطقة عطبرة والتي لم تكن موجودة في العينات المجموعة من مجرى النيل مباشرة في نفس المنطقة.

أخيراً وجد أن العينات المجموعة من الخط الناقل للمياه في منطقة شندي خالية من الجزيئات السامة مثل (NO^{-3} و C≡N) على عكس تلك العينات المجموعة من مجرى النيل مباشرة في نفس المنطقة. أما بالنسبة للعينات المجموعة من الخط الناقل للمياه في منطقة شندي، اشارت النتائج إلى أنه يوجد لها جزيئات (S-S، Aromatic nitrile، UO_2^{+2} و $\nu(C-N)_\beta$) والتي لم تشاهد في العينات المجموعة من مجرى النيل مباشرة في نفس المنطقة.

Contents

Chapter One

Introduction and Basic Concepts

1.1 Introduction

Spectroscopy is the study of the interaction between Electromagnetic Radiation (energy) and matter. And can be used to obtain information about the identity and structure of substances. It is generally involve measurements of two experimental parameters: The energy of the radiation absorbed or emitted by the system and the Intensity of the spectral lines.

Molecular spectroscopy is an essential tool in establishing the nature of substances. It has had an intimate association with the development of various fundamental branches of science, including Physics, Chemistry, Astrophysics, Metrology and Biology, and has also made substantial contributions to advances of technology ranging from industrial processing to monitoring and control engineering.

Molecular spectroscopy has had a long history, which was accelerated by the establishment of quantum mechanics six decades ago. Milestones of this history were the publication of the monumental books by Herzberg, and by Townes and Schawlow, where almost all of the fundamental regularities for molecular electronic, vibrational, rotational and hyperfine spectra as well as their distortions due to inner or external interactions of molecules, and their relations with molecular structures, have been elucidated (Townes, C.H. and Schawlow, A.L., 2013).

However, molecular energy-level structures are extremely complicated compared with those of atoms. As Schawlow put it, a diatomic molecule is a molecule with one atom too many. Although the achievements have been considerable even for large and complicated molecules, it is true that even the knowledge about a

molecule as small and simple as a sodium dimmer is far from satisfying. Until the middle of the 1970's, there were only 5 excited electronic states in Na2 for which the constants had been determined experimentally. The situation was worse for other molecules. Furthermore, to go beyond the mere interest on extremely precise spectral data, it was necessary to analyze dynamic characteristics (Wang, Z.G. and Xia, H.R., 2012).

Notwithstanding the large number of systems studied and the huge amount of data collected, the fundamental limitation of conventional spectroscopy, including spontaneous Raman processes, is linear in nature. Even the modem Fourier spectrometer, that ultimate marriage of spectroscopic and computer technology, cannot help to break through the ultimate spectral resolution of Doppler broadening due to molecular thermal motions. Thus for a long time the hyperfine constants of molecular energy levels were limited to those obtained for low rotational levels in the lowest vibrational level of the electronic ground state by means of microwave spectroscopy; the traditional analyses of the high spectral density of molecular lines in an electronic vibration-rotational band system were so difficult, requiring months for an expert of molecular spectroscopy with the help of a fast computer, that research was confined to a small circle of famous laboratories. Times changed once the laser was introduced into the field of molecular spectroscopy. The relationship between laser spectroscopy and conventional molecular spectroscopy was not, and will not become, one of replacement, but rather of complementarily. Laser molecular spectroscopy has become an inseparable part of modern molecular spectroscopy. It is well known that by using a low-power tunable laser such as a diode laser instead of a conventional light source an expensive spectrometer, which was once the heart of a molecular spectroscopy research laboratory is not required (Wang, Z.G. and Xia, H.R., 2012).

Even if the interaction of molecules with laser radiation is still dominated by linear processes, the obtainable molecular spectra may be incomparable with conventional spectroscopy in terms of 'such aspects as supersensitive and superfast detection, remote sensing, etc., in addition to high spectral resolution.

Nonlinear interaction of molecules with a laser field is the key aspect of laser molecular spectroscopy. The nonlinear uncoupling and nonlinear coupling spectral effect which are introduced are entirely new concepts in molecular spectroscopy. Here the so-called nonlinear uncoupling interaction indicates the process of coherent absorption induced by the incident laser field with negligible reemission. The most important properties of such kinds of processes are the possibilities of Doppler-free spectral resolution and multi photon absorption, promising unprecedented opportunities for the precise and direct measurement of the hyperfine constants of molecular excited electronic states in the optical wavelength region, and for the experimental determination of molecular constants or of other fundamental parameters of high-lying, including traditionally forbidden electronic States and high overtone or combination vibrational levels which used to be inaccessible (Wang, Z.G. and Xia, H.R., 2012).

1.2 Molecular Energy States

Starting from the equation of motion for molecules, we briefly summarize the formulas for molecular energy states and levels, including molecular electronic states, vibration-rotational levels and Rydberg states. We treat the energy-level shifts and splitting due to the intramolecular dynamics and angular-momentum couplings as individual perturbations, and list the selection rules for various molecular transitions.

1.2.1 The Molecular Motion Equation and the Hamiltonian Operator

The Schrodinger equation of a molecule can be written as

$$H\psi = E\psi \qquad (1.1)$$

where H is the total Hamiltonian operator, ψ is the total wave function, and E is the total energy of the molecule.

The total Hamiltonian operator can be expressed as

$$H = H_\circ + H' \qquad (1.2)$$

where $H_\circ$ is the part referring to electronic motion as well as to nuclear vibrations and rotations excluding their mutual interactions, whereas. H' represents the effects of all intramolecular interactions. Therefore, with the Born-Oppenheimer approximation we have

$$H_\circ = H_e + H_v + H_r \qquad (1.3)$$

$$\psi = \psi_e + \psi_v + \psi_r \qquad (1.4)$$

$$E = E_e + E_v + E_r \qquad (1.5)$$

where the subscripts e, v and r refer to electronic, vibrational and rotational, respectively . The corresponding term values of the energy levels can be expressed in the form, noting $T = \frac{E}{hc}$

$$T = T_e + G(V) + F(J) \qquad (1.6)$$

where v and J are the molecular vibrational and rotational quantum numbers, respectively (Huber, K.P., 2013).

1.2.2 Molecular Electronic States

Assume a diatomic molecule to be A - B with n electrons, the mass of an electron to be m and the reduced mass of the two nuclei of the molecule to be

$$\mu = \frac{(m_a m_b)}{m_a + m_b} \qquad (1.7)$$

(m_a and m_b are the masses of the two nuclei).

Neglecting the various above-mentioned interactions, the Schrodinger equation of the diatomic molecule can be written as

$$\left[\frac{-\hbar^2}{2\mu}\nabla^2 - \frac{\hbar^2}{2m}\sum_{i=1}^{n}\nabla_i^{\,2} + V\right]\psi = E\psi \qquad (1.8)$$

The electrons of a diatomic molecule move in the axially symmetrical electric field. The total electronic orbital angular momentum L processes around the molecular axis, as shown in Fig.1.2. The axial component of L is equal to $\frac{M_l h}{2\pi}$ with $M_L = L, L-1, L-2, \ldots, -L$ (1.9)

where L is the quantum number of the orbital angular momentum. If all of the electrons were to change direction, M_L would become $-M_L$ but the energy remains the same. However, the different values of $|M_L|$in (1.8) possess unequal energy. Hence the electronic states are specified by$|M_L|$.

The states with equal absolute value $|M_L|$but opposite signs are so-called degenerate states. The quantum number used to represent $|M_L|$isΛ,

$$\Lambda = |M_L| = 0,1,2,3, \ldots, \qquad (1.10)$$

The molecular electronic states with Λ = 0, 1, 2, 3 … are named as$\Sigma, \Pi, \Delta, \Phi$ states, respectively (Wang, Z.G. and Xia, H.R., 2012).

The general selection rules of the electronic transitions can be listed as

$$\Delta\Lambda = 0, \pm 1$$
$$\Delta S = 0 \qquad (1.11)$$
$$\Delta\Sigma = 0$$
$$\Delta\Omega = 0, \pm 1$$

1.2.3 Molecular Vibrational States

A molecular vibration occurs when atoms in a molecule are in periodic motion while the molecule as a whole has constant translational and rotational motion. The frequency of the periodic motion is known as a vibration frequency, and the typical frequencies of molecular vibrations range from less than 10^{13} to approximately 10^{14} Hz, corresponding to wave numbers of approximately 300 to 3000 cm^{-1}.

In general, a non-linear molecule with N atoms has $3N - 6$ normal modes of vibration, but a *linear* molecule has $3N - 5$ such modes, because rotation about its molecular axis cannot be observed (Landau, L.D. and Lifshitz, E.M., 2013).

A diatomic molecule has one normal mode of vibration. The normal modes of vibration of polyatomic molecules are independent of each other but each normal mode will involve simultaneous vibrations of different parts of the molecule such as different chemical bonds.

A molecular vibration is excited when the molecule absorbs a quantum of energy, E, corresponding to the vibration's frequency, v, according to the relation $E = hv$ (where h is Planck's constant). A fundamental vibration is excited when one such quantum of energy is absorbed by the molecule in its ground state. When two quanta are absorbed the first overtone is excited, and so on to higher overtones.

In the harmonic approximation the potential energy is a quadratic function of the normal coordinates. Solving the Schrödinger wave equation, the energy states for each normal coordinate are given by

$$E = h\left(n + \frac{1}{2}\right)\nu = h\left(n + \frac{1}{2}\right)\frac{1}{2\pi}\sqrt{\frac{k}{m}} \qquad (1.12)$$

where n is a quantum number that can take values of 0, 1, 2 ... In molecular spectroscopy where several types of molecular energy are studied and several quantum numbers are used, this vibrational quantum number is often designated as v (Atkins, P.W., Paula J de 2006).

The difference in energy when n (orν) changes by 1 is therefore equal to $h\nu$, the product of the Planck constant and the vibration frequency derived using classical mechanics.

For a transition from level n to level n+1 due to absorption of a photon, the frequency of the photon is equal to the classical vibration frequency ν (in the harmonic oscillator approximation).

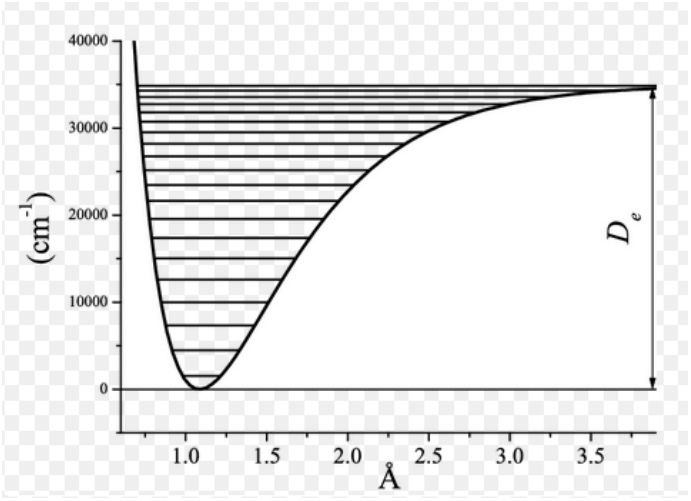

Figure 1.1 Vibmtional energy level scheme in the electronic ground state of diatomic molecule

For a harmonic oscillator transitions are allowed only when the quantum number n changes by one,

$$\Delta n = \pm 1 \qquad (1.13)$$

But this does not apply to an anharmonic oscillator; the observation of overtones is only possible because vibrations are anharmonic. Another consequence of anharmonicity is that transitions such as between states n=2 and n=1 have slightly less energy than transitions between the ground state and first excited state. Such a transition gives rise to a hot band. To describe vibrational levels of anharmonic oscillator, Dunham expansion is used.

1.2.4 Molecular Rotational Levels

Investigating the rotation of a diatomic molecule with the rigid-rotator model, we can solve the angular part of the Schrodinger equation and obtain the level expression for pure rotation (Wang, Z.G. and Xia, H.R., 2012).

$$F_J = BJ(J+1) \qquad (1.14)$$

where B is the constant of rotation, which is

$$B = h(8\pi^2 c I_e)^{-1} \qquad (1.15)$$

For a diatomic molecule

$$I = \frac{m_1 m_2}{m_1 + m_2} d^2 \qquad (1.16)$$

where m_1 and m_2 are the masses of the atoms and d is the distance between them.

For pure rotational transitions the selection rule of the rotational quantum number is

$$\Delta J = \pm 1 \qquad (1.17)$$

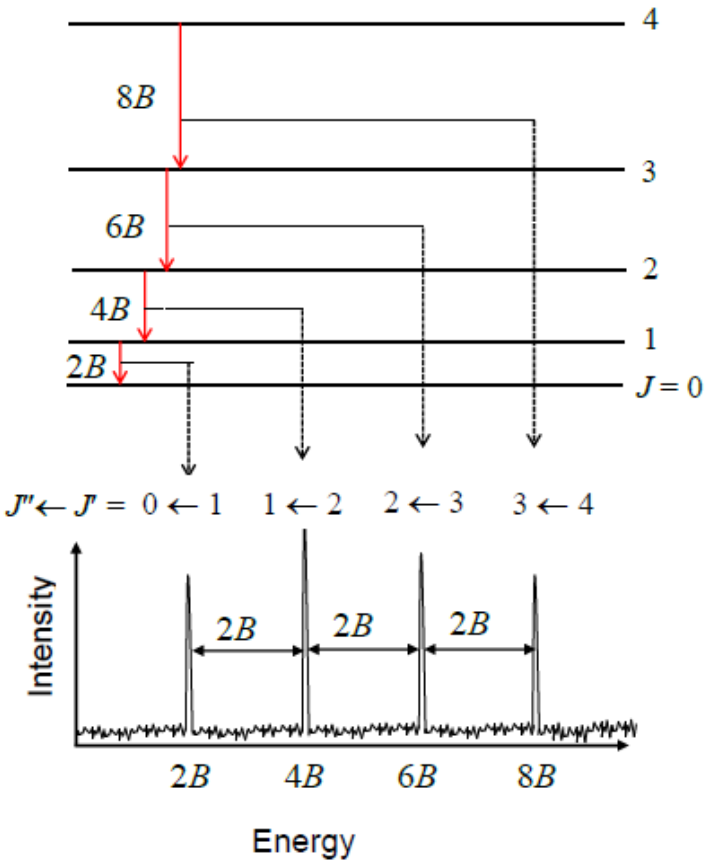

Figure 1.2 Energy levels and line positions calculated in the rigid rotor approximation

1.3 Research Problem

Water pollution is a complex problem for people in Sudan, especially in the northern state. Most population there are supplied by water sources directly from the Nile for drinking and irrigation purposes. As noted recently there have been cases of cancer and renal failure. Water is expected to be one of major and direct cause of these diseases. So this study aims to mapping molecules on Nile water in Northern Sudan.

1.4 Objectives of Research

The objectives of this study are:

Appling laser Raman spectroscopy to mapping molecules on Nile water in Northern Sudan.

Comparison between the spectrum of the samples which took directly from the Nile and that collected from the pipelines after water treated by water treatment plant.

Comparison between the results (the results obtained from this study with the results obtained from other studies).

1.5 Thesis Structure

This thesis consists of four chapters:

Chapter one presents an introduction and Basic Concepts of spectroscopy and literature review. Then chapter two discuses the use of water, surface water and contaminated water. In addition, Laser spectroscopy and the fundamentals and applications of Raman spectroscopy in classical and quantum images, Raman spectrometers, types of Raman spectroscopy, Raman spectroscopy applications. Chapter three covers the practical side, methods of samples collection, Raman setup and procedure. Finally chapter four deals with the obtained results, the analysis of Raman spectra, the discussion of the results, the comparison with other results, conclusions and recommendations.

1.6 Literature Review

In 2007, K. A Vereschagin. et.al, used the Coherent anti-stokes Raman spectroscopy to investigate the collisional broadening of the hydrogen Q branch transitions by water at high temperatures. The CARS spectra re cordedin the channel of the measurement complex were processed as follows. First, temperature estimation was done (temperature range 2500 – 3500 K). For identical values of

temperatures and pressures, the data from another channel on the widths of spectral lines were selected. The standard deviation for a series of temperature measurements was typically 100–200 K, which makes up 3–5% from the measured values of temperatures. They concluded that, the broadening coefficients for hydrogen Q-branch lines are due to collisions with water molecules at temperatures from 2100 up to 3500 K inside a high pressure hydrogen–oxygen combustion chamber (Baer, B.J., et al., 2007).

In 2012 Alison J. Wright and Martin R. Lee they were used Raman spectroscopy to characterized by crusts that develop on sandstone blocks and identify chelating compounds created in complex biomass crusts. The results of this work helped evaluate those scales that must be removed to prevent them Biodegradation of stone and those that must be left intact to protect the stone from other weathering factors.

The samples investigated to date include a suite of 6 sandstone types used in previous study to determine the effects of abrasive cleaning and the use of biocides on biological growth (Young 1997). Since 1993, 144 blocks of stone approximately 5 x 5 x 2 cm in size have been left to weather on a test-rig in Aberdeen (north-east Scotland) with the samples equally divided between north- and south-facing aspects. Four of the sandstone types are dominated by algal growth and 2 are covered by a mixed lichen flora. There is now no apparent difference between untreated blocks and those that were cleaned prior to the start of the trial and the north and south facing subsets support similar biological communities. Initial analysis using Raman spectroscopy shows that the surfaces of all 6 sandstone types are dominated by the biomarker carotene, a substance used to protect cell chloroplasts from photo-oxidation (Alison J. Wright, 2012)

In 2014 Ivana Durickovic and Mario Marchettiuse Raman spectroscopy for water pollution detection, This study shows the relevance of using Raman spectrometry

for the detection and the quantification of several major pollutant families in an aqueous media such as drugs, pesticides or salts coming from fertilizers. commercial products were chosen. For the study on drugs, an analysis was performed on a contraceptive pill based on ethinylestradiol (the hormone present in the majority of contraceptive pills) and a drug based on niflumic acid (predominantly used as an anti-inflammatory agent).

For the family of pesticides, glyphosate was chosen as a reference pesticide because it is on top of the list of the pesticides which are most commonly used.

A highly contaminated water was prepared by the dilution of a pure pollutant in demineralised water and lower contaminations were obtained by diluting this mother solution. For the commercial products, the composition data given by the commercial products was used for a concentration determination during the dilution process.

After analyzing the Raman spectra obtained, they found that the samples contained potassium phosphate and sodium nitrate (Durickovic, I. and Marchetti, M., 2014).

In 2016 Gurvinder Singh Bumbrah, Rakesh Mohan Sharmastudied the developments in the analysis of drugs of abuse and other illicit substances by Raman spectroscopy for forensic purpose. The review covers the brief overview of basic principle and instrumentation of Raman spectroscopy along with selected and recent applications for characterization of drugs of abuse using this technique. These applications show the potential value of Raman spectroscopy in the qualitative and quantitative analysis of trace amounts of drugs of abuse and other illicit substances on different matrices such as cloth, currency notes, fiber etc., without extensive sample preparation in a non-destructive manner.

Raman spectroscopy has established itself as a reliable and non-destructive technique for the qualitative and quantitative analysis of a variety of drugs of abuse and illicit substances of forensic interest. Technique is capable of analyzing solid

and liquid samples quite rapidly and without removing from packaging and thereby maintaining the integrity of forensic samples. The simplification of spectra caused by resonance allows the easy identification of species contained in complex mixtures. However, low sensitivity due to weak Raman signals and strong fluorescence due to impurities or colored packaging material can be very well addressed by combing two developments of the technique namely resonance Raman and surface enhanced Raman spectroscopy (Bumbrah, G.S. and Sharma, R.M., 2016).

In 2016, Nafie A. Almuslet and Mohammed A. Yousif used Raman spectroscopy to identify the components of water wells in the western region of Saudi Arabia. Water wells samples were collected from different areas, distances apart, and close in the depths. The samples were analyzed by LIRA 300 Raman spectrometer. The results showed that the samples contain different materials, beside the water, with different amounts; like: acids, aromatic molecules, salts, amides, alkynes, phenol, ester and sulfonamide (Nafie A. Almuslet and Mohammed A. Yousif, 2016).

In 2017 Nafie A. Almuslet, Mubarak M. Ahmed and Siham M. Hassen used laser Raman Spectroscopy to identify the unstable compounds in three iron oxides. The results obtained showed that the unstable compounds appeared in the spectra of the samples. Characteristic bands of hematite appeared in the spectra of goethite and akaganeite compounds while magnetite compounds appeared in the spectra of hematite. The laser power causes the bands to broaden and to undergo a small shift to lower wavenumbers. Other materials are appeared in spectra of the three samples like disulfide, alkyl disulfide and aliphatic fluoro. Raman spectroscopy proved to be suitable method for the identification of unstable compounds in hematite, goethite and akaganeite and could be used for other materials (Nafie A. Almuslet, et al., 2017).

In 2018 Anamika Mukhopadhyay and Pankaj Dubey Saied that, the effect of dissolved salts on the hydrogen bonded network in water is extremely important to be understood, as it plays an important role in many aspects of structure and dynamics in aqueous solutions. We have undertaken a study of this phenomenon, using NH4Cl (AC) and (NH4)2SO4 (AS), as the salts for influencing the hydrogen bonded network in water. The effects of varying the temperature and concentration in these aqueous solutions of both the salts, on the Raman spectra were studied, over the wavenumber range 50– 4000 cm−1. It was found that at 25 °C, with increasing AS concentration, a monotonic increase in intensity of spectral features on the low wavenumber side (~3200 cm−1 region) of the O–H stretching band was observed, whereas AC showed the opposite effect. A parameter (χstruct) is defined from the spectral data, which indicates that more hydrogen bonded network forms in presence of AS salt compared with AC salt, in aqueous solution. Temperature variation study also reveals that, presence of AC induces a more disordered network in aqueous solutions, than AS. To support these conclusions, we have performed ab initio calculation for the salt ⋯nW species, where n = 1−8, using the MP2/ 6–31+G (d,p) level of theory. Solvent separated ion pair formation has been reported for NH_4^+ and Cl^- ions, whereas NH_4^+ and SO_4 2-ions remain as contact ion pair up to AS ⋯8W cluster. This study helps understand the effect of salt water interaction at the molecular level and may have huge implications in atmospheric physics, geophysics, and ice crystallization (Mukhopadhyay, A. and Dubey, P., 2018).

Chapter Two

Water Structure and Raman Spectroscopy Principles

2.1 Introduction

In this chapter I have attempted to introduce and discuss and summarize the water structure, its importance and its uses. Also I am going to introduce laser in spectroscopy, basic concepts and applications of Raman spectroscopy in classical and quantum images, selection rules, Raman spectrometers, types of Raman spectroscopy and its applications.

2.2 Preface

Within our Solar System, Earth is known as the water planet, and water is an absolute requirement of life. On our planet, the most controlling resource is water, not oil or minerals but water. Its distribution, quantity, availability, and quality are the controls for the development of agriculture, industry, rural, urban, and municipal use. The water-rich areas of the world are truly the richest places on Earth.

There would be little objection to many wasteful uses of water if fresh water of good quality were unlimited; however, the sad fact is that it is not. Only about 3 percent of the total water in the world is fresh water, and most of that is locked in ice caps and glaciers. Just a fraction of Earth's water about 0.3 percent is accessible fresh water, and approximately 98 percent of this amount is stored as groundwater.

The rest is water in streams and lakes, stored in the soil, and in the atmosphere. All of the water on Earth, salty and fresh, is part of the hydrologic cycle that must be studied in great detail locally and worldwide to provide the data needed to properly develop and manage this most valuable resource.

Basic information is needed so that our water resources can be used wisely. We have learned that mismanagement of our water resources will bring on one water crisis after another.

When we turn the faucet on we expect clean water to come out, twenty four hours a day, seven days a week. Our expectations are so high that we have built large dams and associated reservoirs, pumped large quantities of groundwater from aquifers, and constructed intricate water distribution systems to transport water from areas where it is located to where we prefer to live.

We monitor the quality of our water and spend billions of dollars to treat it (DV and as, S.J., Winter, T.C. and Battaglin, W.A., 2002).

2.3 Importance of Water

Water is essential to life. It is part of the physiological process of nutrition and waste removal from cells of all living things. It is one of the controlling factors for biodiversity and the distribution of Earth's varied ecosystems, communities of animals, plants, and bacteria and their interrelated physical and chemical environments. In terrestrial ecosystems, organisms have adapted to large variations in water availability.

Water use by organisms in desert ecosystems is vastly different from those in forest ecosystems. For example, some seeds lie dormant for years in arid climates waiting to be awakened by a rare precipitation event. In contrast, a large oak tree in a temperate climate returns about 4,000 gallons of water a year to the atmosphere. Through the process of transpiration, plants give off moisture largely through their leaves.

Aquatic ecosystems, such as wetlands, streams, and lakes, are especially sensitive to changes in water quality and quantity.

These ecosystems receive sediment, nutrients, and toxic substances that are produced or used within their watershed the land area that drains water to a

stream, river, lake or ocean. As a result, an aquatic ecosystem is indicative of the conditions of the terrestrial habitat in its watershed. Wetland ecosystems provide habitat to a great variety of birds, plants and animals.

These transitional areas between dry and wet habitats help reduce floods and abate water pollution. They also support many recreational activities and commercial fisheries and provide a number of other important functions. Nearly every activity that occurs on land ultimately affects ground waters or surface waters.

Water plays a major role in shaping the land surface of the Earth. Canyons, flood plains, terraces, and watersheds are formed by the action of water flowing across the land surface. As a result, watersheds have many different shapes and sizes . Some contain parts of mountains and hills, and others are nearly flat (DV and as, S.J., Winter, T.C. and Battaglin, W.A., 2002).

2.4 Water Quality

Although it is technically possible to treat water of just about any quality to make it suitable for a public water supply, it is often not economically practical to do so. In some situations, it may be more cost effective to pipe water a considerable distance from a remote, good-quality supply than to treat poor-quality water that is available locally. In some parts of the United States, for example, it is less expensive for some coastal cities to transport fresh water from sources hundreds of miles away than to desalt the ocean water nearby. Elsewhere in the world, however, desalinization must be used because the amount of available fresh water is not sufficient.

The economic concerns associated with drawing on a limited water resource to provide adequate water where several communities need it are often complex. Costs are influenced by the supply and demand among all the parties that have an interest in using the water. Political and legal considerations, such as who

has the rights to the water, also come into play. The costs of the energy needed to operate the treatment plant may fluctuate considerably over the life of the plant.

As water treatment technology becomes more efficient, however, the cost of treating poor-quality sources decreases, making treatment a more attractive option for some communities.

Some of the principal quality factors that must be considered in evaluating the suitability of a water source for use are:

• Excessive turbidity.

• Microbiological contamination.

• Chemical or radiological contamination.

• Undesirable taste, odor, or color.

• Presence of algae growth.

• Water temperature.

The influences of factors on water use and treatability are covered in Water Treatment and Water Quality, other titles in this series (Melissa Valentine, et al., 2010).

2.5 Chemical and Physical Properties of Water

The smallest unit of water is called a molecule. It is made up of two atom of hydrogen and one atom of oxygen, resulting in the familiar chemical term for water H_2O. The chemical makeup of water gives it specific characteristics, such as its density and its ability to dissolve substances.

Water is a polar inorganic compound that is at room temperature a tasteless and odorless liquid, nearly colorless with a hint of blue. This simplest hydrogen chalcogenide is by far the most studied chemical compound and is described as the "universal solvent" for its ability to dissolve many substances (Greenwood, N.N. and Earnshaw, A., 2012).

This allows it to be the "solvent of life". It is the only common substance to exist as a solid, liquid, and gas in normal terrestrial conditions (Reece, Jane B., 2013).

2.6 Polarity and Hydrogen Bonding

Since the water molecule is not linear and the oxygen atom has a higher electro negativity than hydrogen atoms, it is a polar molecule, with an electrical dipole moment: the oxygen atom carries a slight negative charge, whereas the hydrogen atoms are slightly positive. Water is a good polar solvent, that dissolves many salts and hydrophilic organic molecules such as sugars and simple alcohols such as ethanol. Water also dissolves many gases, such as oxygen and carbon dioxide. In addition, many substances in living organisms, such as proteins, DNA and polysaccharides, are dissolved in water. The interactions between water and the subunits of these bio macro molecules shape protein folding, DNA base pairing, and other phenomena crucial to life (hydrophobic effect).

Many organic substances (such as fats and oils and alkanes) are hydrophobic, that is, insoluble in water. Many inorganic substances are insoluble too, including most metal oxides, sulfides, and silicates.

Because of its polarity, a molecule of water in the liquid or solid state can form up to four hydrogen bonds with neighboring molecules. These bonds are the cause of water's high surface tension and capillary forces (Sweeney, D. and Williamson, B., 2006).

The capillary action refers to the tendency of water to move up a narrow tube against the force of gravity. This property is relied upon by all vascular plants, such as trees (jrank, 2013).

The hydrogen bonds are also the reason why the melting and boiling points of water are much higher than those of other analogous compounds like hydrogen

sulfide (H 2S). They also explain its exceptionally high specific heat capacity (about 4.2 J/g/K), heat of fusion (about 333 J/g), heat of vaporization (2257 J/g), and thermal conductivity (between 0.561 and 0.679 W/m/K). These properties make water more effective at moderating Earth's climate, by storing heat and transporting it between the oceans and the atmosphere. The hydrogen bonds of water are of moderate strength, around 23 kJ/mol (compared to a covalent O-H bond at 492 kJ/mol). Of this, it is estimated that 90% of the hydrogen bond is attributable to electrostatics, while the remaining 10% reflects partial covalent character (Isaacs, E.D., et al., 2000).

2.7 Water Quality Standards

Water quality standards are the numeric values or statements that define the acceptable characteristics of our waters and they give us a frame of reference for protecting their quality . For example, to prevent our waters from becoming too acidic or alkaline, states have adopted water quality standards for pH. Although standards may vary slightly from one state to another, a typical standard would require the pH of a particular water body to be within the range of about 6.0 to 8.5- neither too acidic nor too basic. Most states have adopted water quality standards for temperature, dissolved oxygen, turbidity, bacteria, solids, and toxic substances (Kenneth M. Vigil, P.E. 2003).

The water must be free from toxic molecules and chemicals, but if it appears with the test, it should not exceed the permissible limit.

WHO's Guidelines for Drinking-water Quality, set up in Geneva, 1993, are the international reference point for standard setting and drinking-water safety (World Health Organization, 2004).

Table 2.1 WHO Specification for Drinking Water

Property / component	International Standard mg/liter
Color (TCU)	15
Soluble solids	1000
Suspended solids	0
Turbidity (NTU)	5
PH	6.5-8.5
Dissolved oxygen	0
Water shortage	500
Ammonia	0
Ammonium	0
Nitrates	0
Nitrite	0
Phosphorus	0
BOD	0
Sodium	200
Chloride	250
Sulfate	400
Sulphide	0
Fluoride	1.5
Boron	0
Cyanide	0.1
Aluminum	0.2
Arsenic	0.05
Barium	0
Cadmium	0.005

Chromium	0.05
Cobalt	0
Copper	1
Iron	0.3
Lead	0.05
Magnesium	0.1
Mercury	0.001
Nickel	0.01
Selenium	0
Zinc	5
Oil and petroleum	0
Total pesticides	0
Individual pesticides	0
Pesticide	0.03
Dichlorobenzene trichloroethane	1
Hexachlorocyclohexane	3
Methoxy Chlorine	30
Benzene	10
Hexachlorobenzene	0.01
Pentachlorophenol	10
Phenols	0

2.8 Lasers in Spectroscopy

Modern analytical techniques should be highly specific and sensitive enough to identify and quantify an analyte of interest with minimum requirements for sample pretreatment.

There are many of these analytical techniques, I will explain briefly and the most important is Raman spectroscopy is a highly specific technique that enables identification of molecules through their specific molecular fingerprint information as observed in their Raman spectra.

2.8.1 Laser Induced Breakdown Spectroscopy(LIBS)

Laser Induced Breakdown Spectroscopy (LIBS) is not really a new technique. First experiments aimed to detect atomic line emission after the laser induced plasma formation at metal surfaces in air date back to the early eighties (Radziemski, L.J. and Loree, T.R., 1981)

However before considering the technique for quantitative analytical applications, substantialinstrumental and data analyses methods development was required. Due to the intense background plasma emission, dominating the process shortly after the laser pulse, fundamental steps in this directions were achieved in the nineties, with the development of intensified optical multichannel analyzers as detectors, offering the combined possibilities of fine time gating and high spectral resolution, the latter with the coupling to a high resolution monochromator. Since then, the process of laser ablation at high laser power has been studied in detail in order to establish the fundamentals of the technique, especially in relation to the need of retaining the sample stoichiometry during surface evaporation and the occurrence of local thermal equilibrium conditions in plasma for selected time windows.

The laser interaction with matter always involves an energy exchange. Once a laserbeam is focused onto a dense matter, nearby a surface, the laser energy can be partiallyreflected or scattered at the same wavelength, re-emitted at different

wavelengths, absorbed or transmitted in crossing the surface. The interaction of a pulsed laser beam with the surface may lead to it a partial evaporation originating a process known as laser induced ablation, whose main characteristics are:

Localized heating at the surface, both in space and in time; Fast process evolution, with a complete cycle shorter than 10 ms (for pulse width<100 ns) (Amoruso, et al., 1999).

For high irradiances (e.g. >1MW/cm , depending on the target composition) the evaporation composition) the evaporation occurs with a plasma formation, involving several successive processes such as: surface melting with hydrodynamic flow, vaporization, vaporionization, surrounding and evaporating gas breakdown, free electron acceleration within the evaporated cloud, plasma heating.

The plasma growth and decay implies: expansion, shock waves formation and propagation, deceleration of free electrons with inverse Bremsstrahlung emission, collisions in the gas cloud with excitation and relaxation of atoms/ions, chemical recombination, radiative recombination.

Occasionally conditions associated to a Local Thermal Equilibrium (LTE) can occur, whenever electrons, atoms and ions in the plasma are associated to the same temperature. The LTE is a dynamic status reached for plasma parameters slowly varying in a suitable temporal range, during the plasma relaxation. Initially, the plasma temperature is very high (typically T >30000K), and auto-ionization accompanied by a continuum emission spectrum is dominant (Russo, R.E., et al., 2002).

Fast collisional processes bring the plasma to conditions of LTE, where the electrons have a Maxwell energy distribution, all the species have the same temperature, the population of energy levels follow a Boltzmann distribution, and Saha equation describes the concentration ratio among the same species at different degrees of ionization. Upon LTE conditions, characteristic line emission spectra

are detected mostly from the atomic and first ionic excited species produced. Note that a high electron density is needed to reach LTE: electron collisional rates must exceed radiative rates by at least one order of magnitude (Griem, H.R., 2005).

Further plasma cooling and recombination cause plasma departure from LTE. In its final stages the process is characterized by cluster and nanoparticles ejection in the dark slow expanding tail of the plume (Dolgaev, S.I., et al., 2002).

During the laser ablation at high energy densities, accompanied by the plasma formation which gives rise to line emissions recorded in LIBS, the bright plume is observed in combination with the formation of a crater at the surface. In the evaporation atoms are ejected perpendicularly to the sample surface, the enhancement along this direction is due to crater shape which may convey material towards laser direction, thereby increasing excitation. In summary, LIBS emission intensity is maximum for normal incidence, and the central plume region has the most intense emission, due to the higher density of the emitting species.

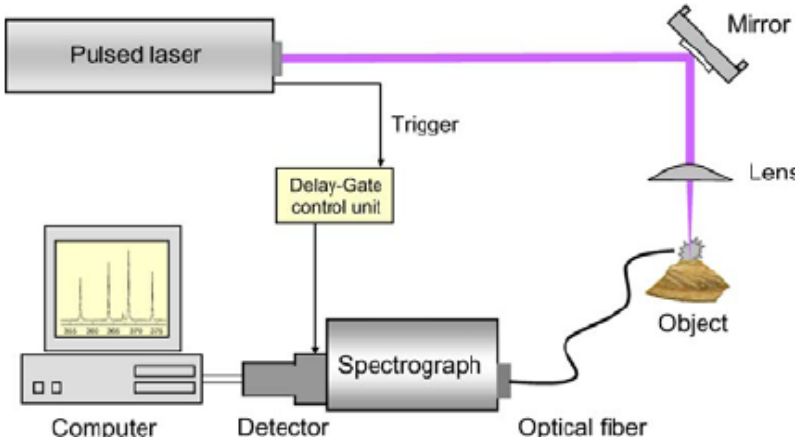

Figure 2.1 Set-up for LIBS

2.8.2 Laser Induced Fluorescence Spectroscopy (LIF)

Laser-induced fluorescence (LIF) or laser-stimulated fluorescence (LSF) is a spectroscopic method in which an atom or molecule is excited to a higher energy level by the absorption of laser light followed by spontaneous emission of light. It was first reported by Zare and coworkers in 1968.

LIF is used for studying structure of molecules, detection of selective species and flow visualization and measurements. The wavelength is often selected to be the one at which the species has its largest cross section. The excited species will after some time, usually in the order of few nanoseconds to microseconds, de-excite and emit light at a wavelength longer than the excitation wavelength. This fluorescent light is typically recorded with a photomultiplier tube (PMT) or filtered photodiodes.

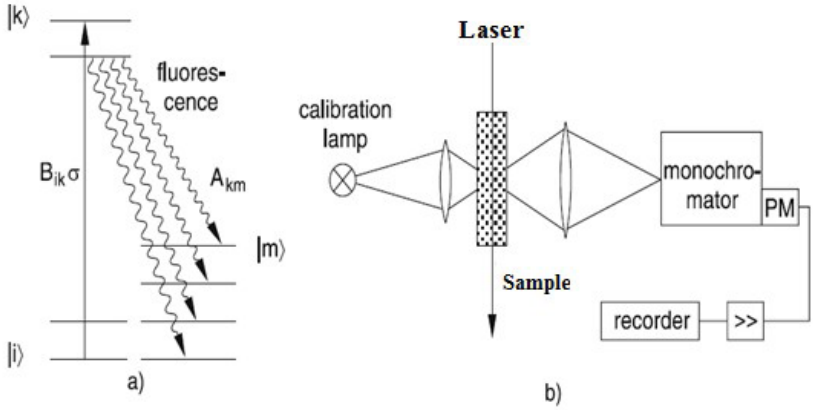

Figure 2.2 Laser-induced fluorescence: (a) level scheme and (b) experimental arrangement for measuring LIF spectra.

Like for opto-acoustic detection and CRDS, this technique is only suitable for point measurements. It is limited to those species which have absorption/emission bands in the UV/Visible. A laser is not necessary, as lamps (like mercury lamp, a very cheap source) can fulfill the measurement requirements (Richard W. Solarz; Jeffrey A. Paisner, 1986.)

2.8.3 Laser Absorption Spectroscopy

Absorption spectroscopy is a simple and intuitive technique that offers fewer opportunities for mistakes than more complicated strategies. Therefore, direct-absorption is very attractive when absorption signals are large and the signal-to-noise ratio is high. In direct-absorption, the laser wavelength is tuned over a large wavelength range in order to capture the entire absorption feature. The transmitted light is then attenuated as the wavelength is scanned across an absorption feature of the test gas. The relationship between the ratio of transmitted to incident light and the thermo physical properties of the absorbing gas is given by Beer's Law, which gives by equation below

$$\left(\frac{I_t}{I_\circ}\right)_{\nu} = e^{-\alpha\nu} \qquad (2.1)$$

The left-hand side of equation (2.1) is the ratio of transmitted I_t to incident $I_\circ$ light intensity at optical frequency ν and inside the exponential on the right-hand side is the absorbance at frequency ν, αν. Simulations of incident and transmitted laser intensities are shown in Fig. 2.3a. In practice, the transmitted intensity is usually measured, and the incident intensity is then inferred by fitting a baseline curve through the non-absorbing region of the laser scan (e.g., the incident intensity in Fig. 2.3a is accurately recovered by fitting a sinusoid to the non-absorbing regions of the transmitted intensity curve) (Schultz, I., 2014)

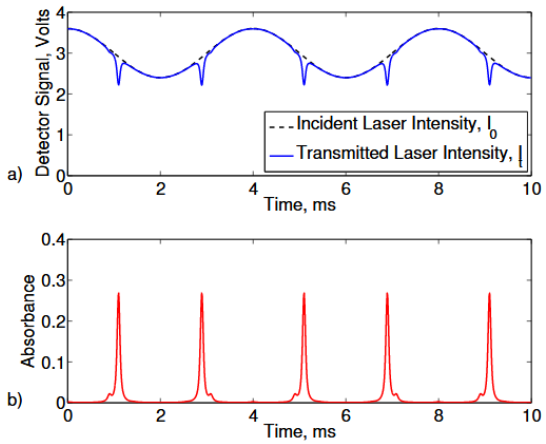

Figure 2.3 Simulated laser scans to measure direct-absorption line

2.9 Basic Theory of Raman Spectroscopy

Raman spectroscopy is a spectroscopic technique based on inelastic scattering of monochromatic light, usually from a laser source. The dominant in Raman scattering is Rayleigh and the very small amount of Raman scattered light. The induced dipole moment occurs as a result of the molecular polarizability, where the polarizability is the change and deformability of the electron cloud about the molecule by an external radiation.

A very small amount of Raman scattered are Stokes and anti-Stokes. Molecules initially in the ground vibrational state (m) excited to virtual states, then return back to vibrational excited state (n) give rise to Stokes Raman scattering $hc(\nu_L - \nu_m)$, molecules initially in vibrational excited state (n) excited to virtual states, then return back to ground vibrational state (m) give rise to anti-Stokes Raman scattering$hc(\nu_L + \nu_m)$. The intensity ratio of the Stokes relative to the anti-Stokes Raman bands is governed by the absolute temperature of the sample, and the energy difference between the ground and excited vibrational states. The Stokes Raman lines are much more intense than anti-Stokes, since at ambient temperature

most molecules are found in the ground state. Figure (2.4) describes Raman Effect (Peter Larkin, 2011).

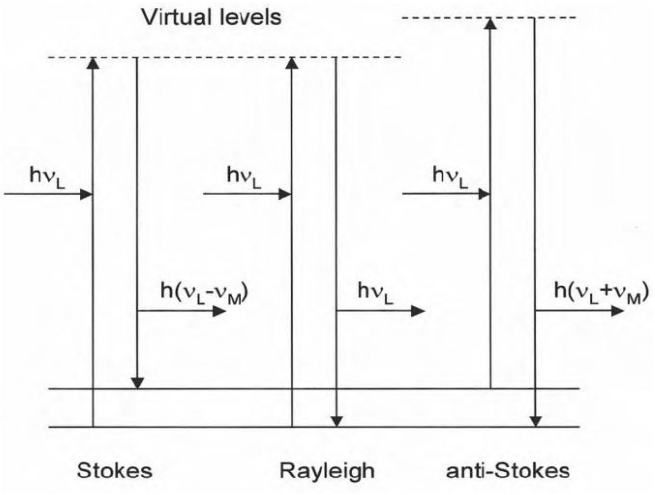

Figure 2.4 The diagram The energy diagram of a molecule showing the Raman scattering

2.9.1 Stokes and Anti-stokes Line

In order for a molecule to exhibit the Raman effect, the incident light must induce a dipole-moment change or a change in molecular polarizability. An electron with certain vibrational modes can couple with the incident-light photon and lead to scattered photons with altered frequency. The scattered light contains a small portion of light due to Raman scattering in addition to that due to normal Rayleigh scattering (same frequency as the incident light). The Raman scattering contains both a Stokes line and an anti-Stokes line; their frequencies correspond to the sum and the difference of frequency of the incident light and the allowed molecular vibrational frequencies. When photons interact with a molecule, some of their energy can be converted into various modes of vibrations of the molecule. As seen in Figure 1.6, the scattered light loses energy equivalent to the energy given to molecular vibrations (Stokes Raman effect). If the energy is transferred to the

scattering light from a molecule, then the scattered light has more energy than the original incident light (anti-Stokes Raman effect). This requires that the scattering molecule already be in an excited state. For typical applications this is seldom the case; therefore, Stokes Raman scattering is much stronger than anti-Stokes scattering. Only a small fraction of photons are scattered by Raman scattering, so Raman lines are usually very weak (only 10-6 of the intensity of the Rayleigh line). The majority of the scattered light is the same as the original incident light in terms of photon energy. This is why a laser is used as a light source: it is an intense, monochromatic source of light and produces more scattered photons (Tu, A.T., 1982).

2.9.2 Raman Scattering

The Raman scattering effect arises from the interaction of the incident light with the electrons in the illuminated molecule. In nonresonance Raman scattering, the energy of the incident light is not sufficient to excite the molecule to a higher electronic level. Instead, Raman scattering results in changing the molecule from its initial vibrational state to a different vibrational state as in Figure (2.5).

The energy diagram of a molecule showing the origin of Raman scattering (nonresonance Raman effect). Note the different mechanisms of the Stokes and anti-Stokes effects; yet their energy differences (Raman shifts) are the same. The net effect is either an increase or decrease in the vibrational-energy level of a molecule. The molecule is momentarily elevated to a higher energy level (virtual state) but it never reaches an electronic excited state.

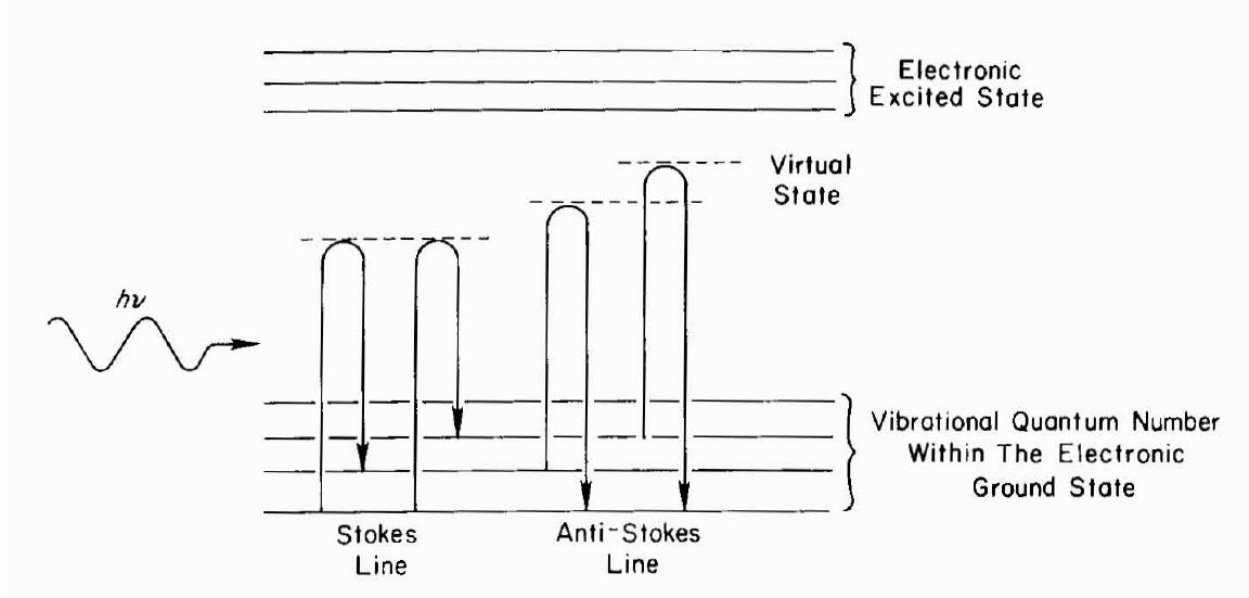

Figure 2.5 Raman Scattering

The energy diagram of a molecule showing the origin of Raman scattering (nonresonance Raman effect). Note the different mechanisms of the Stokes and anti-Stokes effects; yet their energy differences (Raman shifts) are the same. The net effect is either an increase or decrease in the vibrational-energy level of a molecule. The molecule is momentarily elevated to a higher energy level (virtual state) but it never reaches an electronic excited state (Tu, A.T., 1982).

2.10 Selection Rules for Raman Spectra

The basic selection rule is that Raman scattering arises from a change in polarizability in the molecule. As we shall demonstrate later, this means that symmetric vibrations will give the most intense Raman scattering. This is in complete contrast to infrared absorption where a dipole change in the molecule gives intensity and, at a very simple level, this means asymmetric rather than symmetric vibrations will be intense (Edwards HG., 2005).

To determine if the vibration is active in the Raman spectra, the selection rules

must be applied to each normal vibration. Since the origins of Raman spectra are markedly different than IR spectroscopy, their selection rules are also distinctively different. According to quantum mechanics a vibration is Raman active if the polarizability is changed during the vibration (Ferraro, J.R., 2003).

To discuss Raman activity, let us consider the nature of the polarizability. When a molecule is placed in an electric field (laser beam), it suffers distortion since the positively charged nuclei are attracted toward the negative pole, and electrons toward the positive pole (Figure 2.3). This charge separation produces an induced dipole moment (P) given by

$$P = \alpha E \qquad (2.2)$$

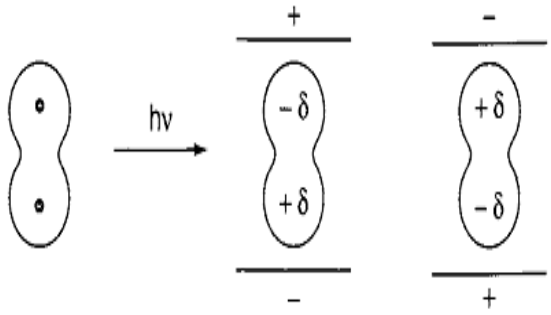

Figure 2.6 Polarization of a diatomic molecule in an electric field.

In actual molecules, such a simple relationship does not hold since both ***P*** and ***E*** are vectors consisting of three components in the x, y and z directions Thus, Eq. (2.2) must be written as

$$\begin{aligned} p_x &= \alpha_{xx}E_X \quad \alpha_{xY}E_Y \quad \alpha_{xZ}E_Z \\ p_y &= \alpha_{Yx}E_X \quad \alpha_{YY}E_Y \quad \alpha_{YZ}E_Z \\ p_z &= \alpha_{Zx}E_X \quad \alpha_{ZY}E_Y \quad \alpha_{ZZ}E_Z \end{aligned} \qquad (2.3)$$

In matrix form this is written,

$$\begin{bmatrix} P_x \\ P_y \\ P_z \end{bmatrix} = \begin{bmatrix} \alpha_{xx} & \alpha_{xy} & \alpha_{xz} \\ \alpha_{yx} & \alpha_{yy} & \alpha_{yz} \\ \alpha_{zx} & \alpha_{zy} & \alpha_{zz} \end{bmatrix} \begin{bmatrix} E_X \\ E_Y \\ E_Z \end{bmatrix}$$

The first matrix on the right-hand side is called the polarizability tensor. In normal Raman scattering, this tensor is symmetric.

$$\alpha_{xy} = \alpha_{yz}\ ,\ \alpha_{xz} = \alpha_{zx} \text{ and } \alpha_{yz} = \alpha_{zy} \quad (2.4)$$

According to quantum mechanics, the vibration is Raman-active if one of these components of the polarizability tensor is changed during the vibration. In the case of small molecules, it is easy to see whether or not the polarizability changes during the vibration. Consider diatomic molecules such as H_2or linear molecules such as CO_2 Their electron clouds have an elongated water melon like shape with circular cross-sections. In these molecules, the electrons are more polarizable (a larger α) along the chemical bond than in the direction perpendicular to it. If we plotα_i(α in the *i*-direction) from the center of gravity in all directions, we end up with a three- dimensional surface. Conventionally, we plot $^1/_{\sqrt{\alpha_i}}$ rather than α_{ij}itself and call the resulting three-dimensional body a polarizability ellipsoid. Figure (2.7) shows the changes of such an ellipsoid during the vibrations of the CO_2 molecule. In terms of the polarizability ellipsoid, the vibration is Raman-active if the size, shape or orientation changes during the normal vibration.

The size of the ellipsoid is changing in $\upsilon_1$vibration and $\upsilon_3$vibration, although the diagonal elements$\alpha_{xx}, \alpha_{yy}\ and\ \alpha_{zz}$**)** are changing simultaneously. Thus, it is Raman-active. The difference between the υ_1 and υ_3 is shown in Figure (2.8).

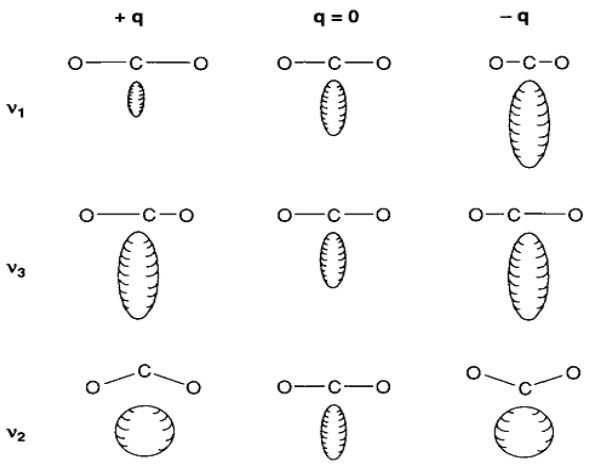

Figure 2.7 Changes Polarizability ellipsoid for different normal vibration modes of CO2.

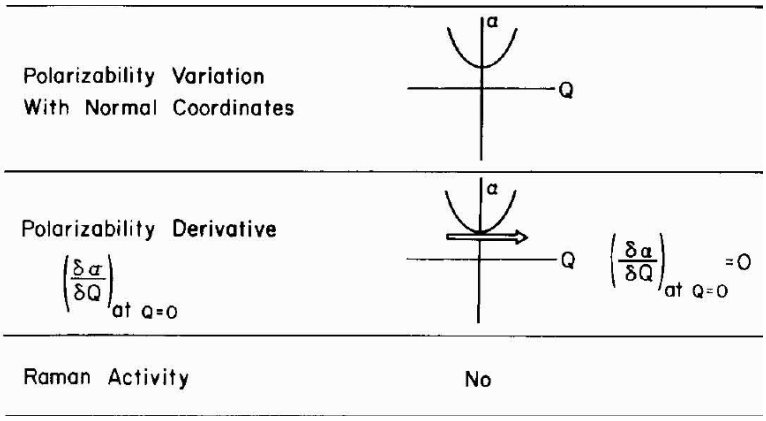

(ν_1)

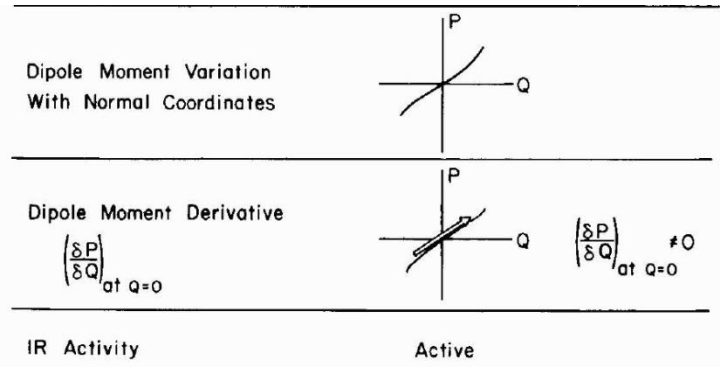

(ν_3)

Figure 2.8 Difference between ν_1 and ν_3 vibrations in CO_2 molecule.

Figure (2.9) illustrates the changes in the polarizability ellipsoid during the normal vibrations of the H_2O molecule. Its ν_1 vibration is Raman-active, as is the ν_3 vibration of CO_2. The υ_2 vibration is also Raman-active because the shape of the ellipsoid is different at + q and − q. In terms of the polarizability tensor, α_{xx}, $\alpha_{yy}$and α_{zz} are all changing with different rates. Finally, the υ_3 vibration is Raman active because the orientation of the ellipsoid is changing during the vibration (Ferraro, J.R., 2003).

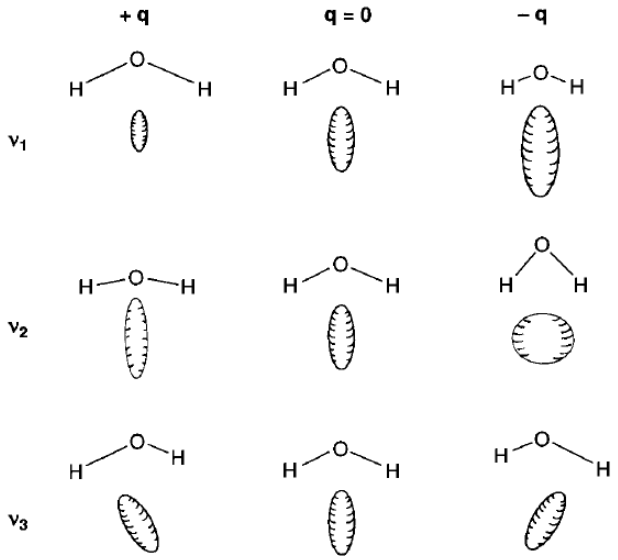

Figure 2.9 Changes in polarizability ellipsoid during normal vibrations of H_2O molecule.

2.11 Raman Spectroscopy Types

Several variations of Raman spectroscopy have been developed. The usual purpose is to enhance the sensitivity, some of these species are the following:

2.11.1 Linear Laser Raman Spectroscopy

The scattering cross sections in spontaneous Raman spectroscopy are very small, typically on the order of 10-30 cm^2. The experimental problems of detecting weak signals in the presence of intense background radiation are by no means trivial. The achievable signal-to-noise ratio depends both on the pump intensity and on the

sensitivity of the detector. Recent years have brought remarkable progress on the source as well as on the detector side. The incident light intensity can be greatly enhanced by using multiple reflection cells, intracavity techniques, or a combination of both. Figure (2.10) depicts as an example of such advanced equipment a Raman spectrometer with a multiple reflection Raman cell inside the resonator of an argon laser. The laser can be tuned by the Brewster prism with reflecting backside (LP + M) to the different laser lines. A sophisticated system of mirrors CM collects the scattered light, which is further imaged by the lens L1 onto the entrance slit S of the spectrometer. A Dove prism DP turns the image of the line source by 90◦ to make it parallel to the entrance slit as shown in Figure (2.10) (W. Demtroder,2008)

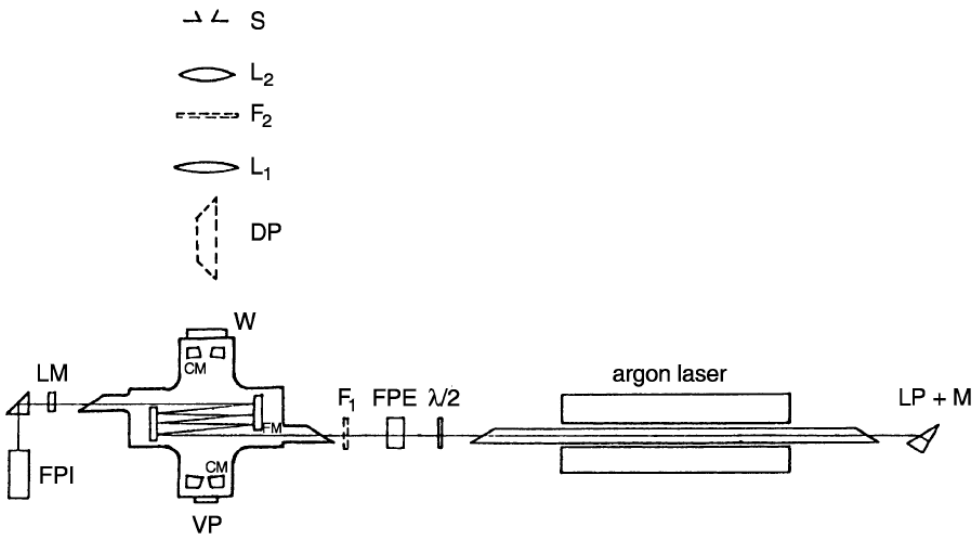

Figure 2.10 Raman spectroscopy with an argon laser: CM=multiple reflection four-mirror system for efficient collection of scattered light; LM= laser resonator mirror; DP= Dove prism, which turns the image of the horizontal interaction plane by 90◦ in order to match it to the vertical entrance slit S of the spectrograph; FPE=Fabry-Perot etalon to enforce single-mode operation of the argon laser; LP= Littrow prism for line selection.

2.11.2 Nonlinear Raman Spectroscopy

When the intensity of the incident light wave becomes sufficiently large, the induced oscillation of the electron cloud surpasses the linear range. This implies that the induced dipole moments p of the molecules is no longer proportional to the electric field E and we have to generalize. The function p (E) can be expanded into a power series of E_n (n = 0, 1, 2, . . .),which is generally written as:

$$p(E) = \mu + \tilde{\alpha}E + \tilde{\beta}E \cdot E + \tilde{\gamma}E \cdot E \cdot E \quad (2.5)$$

where $\tilde{\alpha}$ is the polarizability tensor, $\tilde{\beta}$ is named hyper-polarizability, and $\tilde{\gamma}$ is called the second hyper polarizability. The quantities α, β, and γ are tensors of rank two, three, and four, respectively.

In component notation (i = x, y, z) written as:

$$p_i(E) = \mu_i + \Sigma_k \alpha_{ik}E_k + \Sigma_k \Sigma_j \beta_{ikj} E_k E_j + \Sigma_k \Sigma_j \Sigma_l \gamma_{ikjl} E_k E_j E_l \quad (2.6)$$

This gives for the polarization P = N p of a medium with N oriented dipoles Pi (E) = ε_0) $\chi_i + \Sigma_k \chi_{ik}Ek + \Sigma_{k,j} \chi_{ikj} E_k E_j + . . .)$ (2.7) For sufficiently small electric field amplitudes E the nonlinear terms can be neglected, and we then obtain for the linear Raman spectroscopy (W. Demtroder, 2008).

2.11.3 High-Pressure Raman Spectroscopy

Subjecting various types of matter to high external pressure, and utilizing a spectroscopic technique as the diagnostic tool to determine the changes that have occurred, has proven very successful. Infrared and Raman spectroscopies have been the most useful of the diagnostic tools utilized. Valuable information about intermolecular interactions, phase transitions, structural changes, vibrational assignments and conversions of insulators (semiconductors) to metals is obtainable when matter is subjected to pressure. Pressure-induced frequency shifts are often accompanied by intensity changes and can be used to identify the nature of vibrations and provide correct vibrational assignments (1). A diamond anvil cell (DAC) capable of reaching 5.7 mega bar pressures and ~4,000°K temperature, has

been developed, which allows studies to be made concerning the behavior of various minerals occurring in the depths of the earth (2). Since the core-mantle interface has a pressure of ~ 1.6 Mbar* and 3,000-4,000 K, simulation of core-mantle reactions is possible.

The pressure technique involves a pressure device (DAC) that can transmit the pressure to the sample under study. If spectroscopic methods are chosen for diagnostic purposes, it is a requirement to use windows on the pressure device that are hard and transmit the irradiating light in the particular wavelength of the electromagnetic spectrum being studied. The window of choice for IR and Raman studies is Type IIa diamond. It is the hardest material known and is transmissive for laser Raman studies. Additionally, it is an excellent thermal conductor as well. The pressure device must be compact and fit into the sample compartment of the spectrometer. The DAC fulfills all of these criteria and has been extensively used since its discovery by Weir and Van Valkenburg in 1959. The interface to the Raman spectrometer is readily accomplished (unlike the IR experiment where beam condensers are required in the dispersive instrument, although presently this requirement is unnecessary in the Raman/DAC experiment), and normal commercial Raman instrumentation can be used. Pressure calibration is necessary in pressure work, and this is accomplished by incorporating a small ruby crystal with the sample under study. The Ruby scale was developed by the National Bureau of Standards (now the NIST) in 1972, and the sharp Ruby Ri fluorescent line has been calibrated vs. pressure by NIST, and is suitable even up to megabar pressures . Further details on the Ruby scale are provided in the following section on instrumentation (Ferraro, J.R., 2003).

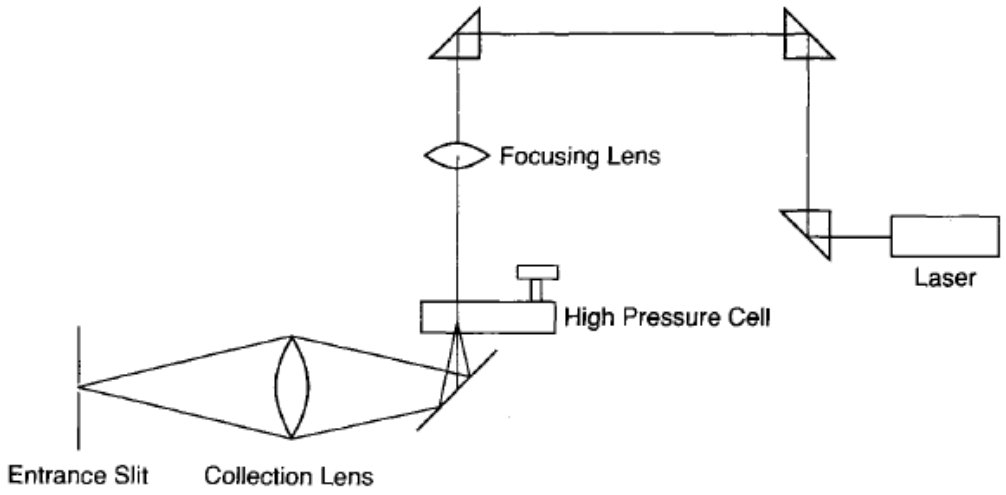

Figure 2.11 Detail of the scattering geometry in laser Raman D AC experiment

2.11.4 Raman Microscopy

Raman microscopy was developed in the 1970s. Delhaye in 1975 made the first micro Raman measurement. The technique provides the capability of obtaining analytical-quality Raman spectra with 1 μm spatial resolution using samples in the picogram range. Commercial instruments are available.

The major limitations in the design of a Raman microprobe are related to the feeble Raman effect and the minute sample size. It is necessary to optimize the Raman signal, and this is accomplished by taking care in the development of the fore optical configuration to provide a high numerical operative and detector system.

The fore optical configuration is extremely important in optimization of the Raman microprobe. A high numerical aperture (NA) is necessary to collect the light scattered over a large solid angle to assure that more Raman scattered light from the sample is detected. A large-aperture collector is used, which minimizes elastic and inelastic scattering from the substrate. The substrate must have a weak Raman or fluorescence spectrum in the region of interest.

Periclase (MgO) can be used as the substrate, although glass slides are routinely used. It has no Raman spectrum and has good thermal properties. A microscope glass slide can be used in some cases. The substrate must be optically polished to provide visible observation of the micro-sized crystal. Additionally, it is important to align the excitation beam onto the substrate to prevent specular reflectance* from entering the Raman scattering path. A spatial filter is used to minimize other sources of spectral interferences. The design of the microprobe is made to provide totally independent optical paths for the excitation radiation and the scattered radiation, and the two paths are then coupled by the scattering properties of the particle being studied. For monochannel instruments an efficient micro analyzer is necessary to provide enough stability to allow the measurement to be made, especially for long periods of time (F. Adar, 1988).

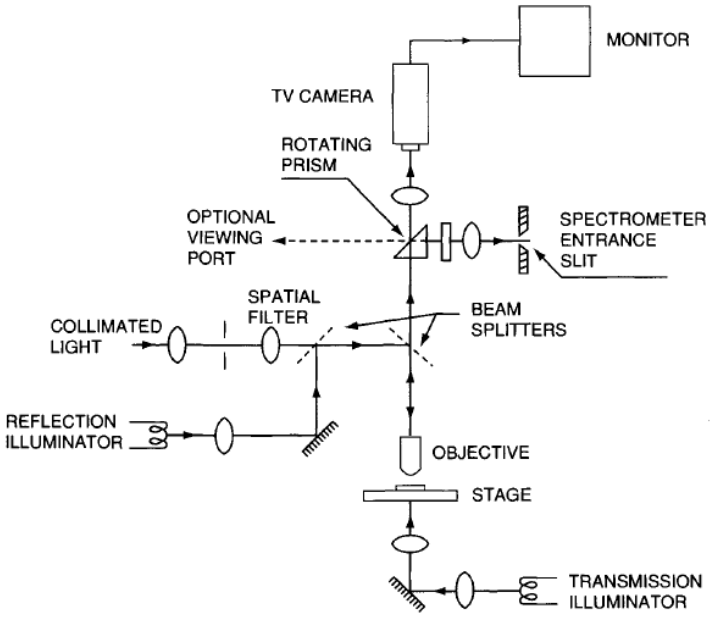

Figure 2.12 Optical path for laser input optics and transfer of the Raman signal to the monochromator for microprobe sampling

2.11.5 Surface-Enhanced Raman Spectroscopy (SERS)

Surface-enhanced Raman scattering (SERS) spectroscopy is based on the enormous enhancement of Raman scattering of molecules adsorbed on suitable

metallic (mainly silver and gold) nanostructures. Two mechanisms contribute to the total enhancement: the electromagnetic one based on resonance excitations of surface plasmons in the metal and the chemical (or molecular) one increasing the polarizability of the molecule. Average enhancement factors are about 104-106 but even values about 10^{11} can be achieved in some cases. This chapter will briefly introduce the basics of SERS theory and some experimental aspects of SERS (choice of metal, distance dependence, selection rules, enhancement factors, "hot spots", single-molecule SERS, resonant SERS). The SERS substrate plays a key role in any SERS application. An overview of SERS-active substrates employed in bioanalytical, biomolecular and medical SERS applications and their properties will be discussed. It includes nanoparticles in suspension, nanoparticles assembled and immobilized on solid substrates (bottom-up approach) and nanostructures fabricated directly on solid substrate (top-down approach). The related enhancing techniques (tip-enhanced RS-TERS, shell-isolated nanoparticles-enhanced Raman scattering-SHINERS, surface-enhanced infrared absorption-SEIRA and surface-enhanced fluorescence-SEF) will also be presented.

The magnitude of the induced dipole moment μ_{ind}, which characterizes the RS effect, is given by a product of the molecular polarizability $\alpha_{molecule}$ and the local electric field E_{loc} of the frequency ω_{inc} demonstrating two possible ways of enhancing RS.1 Interaction of the molecule with a rough metal surface must enhance either E_{loc} or $\alpha_{molecule}$. Thus, the SERS enhancing mechanism is traditionally separated into two main multiplicative contributions: EM and chemical or molecular (Marek Procházka, 2016).

2.11.6 Raman Imaging Spectrometry

Spectra images consist of spectra measured at each spatial location on a sample. They are often referred to as hyper spectral images or a spectral data cube. In the case of Raman images, Raman spectra are measured at the various spatial

locations. After all of the data are collected, it is possible to display individual Raman spectra for each spatial location or to display a false color image based on the intensities at a selected Raman frequency. In the latter representation, the intensities at a selected Raman frequency for each of the spatial locations are assigned to a color correlating to the magnitude of the scattering intensity. For example, low intensities might be assigned to dark blue and high intensities to red with the in-between spectral colors correlating to the medium intensities. A false color image at a selected frequency is often referred to as an image slice of the data cube. The ability to obtain Raman images of chemical and biological samples is of great importance to the scientific community. The improvements and increased use of charge couple devices (CCD) for detection of Raman spectra has made such measurements practical. To obtain an image at a certain Raman frequency, a filter corresponding to the Raman shift could be placed in front of the CCD camera. The observed intensities of the light transmitted by the filter are then converted to a false color image and displayed. However, to obtain a full Raman spectrum at each of the pixels it is necessary to scan each of the spectra at each spatial location. Ideally, one should scan all of the spectra (i.e., at each of the pixels) at the same time, otherwise the measurements would require excessive observation times (Ferraro, J.R., 2003).

2.12 Raman Applications

Raman spectroscopy is used in chemistry to identify molecules and study chemical bonding and intramolecular bonds. Because vibrational frequencies are specific to a molecule's chemical bonds and symmetry (the fingerprint region of organic molecules is in the wavenumber range 500-1500 cm^{-1}), (Clark, J., 2000) Raman provides a fingerprint to identify molecules. For instance, Raman and IR spectra were used to determine the vibrational frequencies of SiO, Si_2O_2,and Si_3O_3 on the

basis of normal coordinate analyses. Raman is also used to study the addition of a substrate to an enzyme (Friesen, M., et al.,1999).

In solid-state physics, Raman spectroscopy is used to characterize materials, measure temperature, and find the crystallographic orientation of a sample. As with single molecules, a solid material can be identified by characteristic phonon modes. Information on the population of a phonon mode is given by the ratio of the Stokes and anti-Stokes intensity of the spontaneous Raman signal. Raman spectroscopy can also be used to observe other low frequency excitations of a solid, such as plasmons, magnons, and superconducting gap excitations. Distributed temperature sensing (DTS) uses the Raman-shifted backscatter from laser pulses to determine the temperature along optical fibers. The orientation of an anisotropic crystal can be found from the polarization of Raman-scattered light with respect to the crystal and the polarization of the laser light, if the crystal structure's point group is known.

In nanotechnology, a Raman microscope can be used to analyze nanowires to better understand their structures, and the radial breathing mode of carbon nanotubes is commonly used to evaluate their diameter.

Raman active fibers, such as aramid and carbon, have vibrational modes that show a shift in Raman frequency with applied stress. Polypropylene fibers exhibit similar shifts.

In solid state chemistry and the bio-pharmaceutical industry, Raman spectroscopy can be used to not only identify active pharmaceutical ingredients (APIs), but to identify their polymorphic forms, if more than one exist. For example, the drug Cayston (aztreonam), marketed by Gilead Sciences for cystic fibrosis, can be identified and characterized by IR and Raman spectroscopy. Using the correct

polymorphic form in bio-pharmaceutical formulations is critical, since different forms have different physical properties, like solubility and melting point.

Raman spectroscopy has a wide variety of applications in biology and medicine. It has helped confirm the existence of low-frequency phonons in proteins and DNA,(Urabe, H., et al., 1983) promoting studies of low-frequency collective motion in proteins and DNA and their biological functions. Raman reporter molecules with olefin or alkyne moieties are being developed for tissue imaging with SERS-labeled antibodies (Schlücker, S., et al. 2011).

Raman spectroscopy has also been used as a noninvasive technique for real-time, in situ biochemical characterization of wounds. Multivariate analysis of Raman spectra has enabled development of a quantitative measure for wound healing progress (Jain, R., et al., 2014).

Spatially offset Raman spectroscopy (SORS), which is less sensitive to surface layers than conventional Raman, can be used to discover counterfeit drugs without opening their packaging, and to non-invasively study biological tissue. A huge reason why Raman spectroscopy is so useful in biological applications is because its results often do not face interference from water molecules, due to the fact that they have permanent dipole moments, and as a result, the Raman scattering cannot be picked up on. This is a large advantage, specifically in biological applications (Butler, H.J., et al., 2016).

Raman spectroscopy also has a wide usage for studying biominerals. Lastly, Raman gas analyzers have many practical applications, including real-time monitoring of anesthetic and respiratory gas mixtures during surgery.

Raman spectroscopy is an efficient and non-destructive way to investigate works of art (Vandenabeele, P., et al., 2007). Identifying individual pigments in paintings

and their degradation products provides insight into the working method of the artist. It also gives information about the original state of the painting in cases where the pigments degraded with age. In addition to paintings, Raman spectroscopy can be used to investigate the chemical composition of historical documents which can provide insight about the social and economic conditions when they were created. It also offers a noninvasive way to determine the best method of preservation or conservation of such materials.

Raman spectroscopy has been used in several research projects as a means to detect explosives from a safe distance using laser beams (Vogel, B., 2008).

Raman Spectroscopy is being further developed so it could be used in the clinical setting. Raman4Clinic is a European organization that is working on incorporating Raman Spectroscopy techniques in the medical field. They are currently working on different projects, one of them being monitoring cancer using bodily fluids such as urine and blood samples which are easily accessible. This technique would be less stressful on the patients than constantly having to take biopsies which are not always risk free.

Chapter Three

Materials and Methods

3.1 Introduction

Experimental part including the materials, equipments and methods have been described in this chapter.

3.2 Materials

In this work, ten samples of surface water were collected from five areas in the northern state (Halfa, Abry, Abuhamd, Atbara and Shandy), These areas cover most of the area of northern Sudan, where the north begin with Shandy and ends with Halfa. Northern Sudan also includes the biggest part of the Nile. figure 2 shows the map of areas which samples were taken from. Two samples were collected from each region, one from the Nile directly and the other from the water line after purification.

The ten samples were put in small sterilized plastic tanks to ensure that water is not contaminated by any external additives.

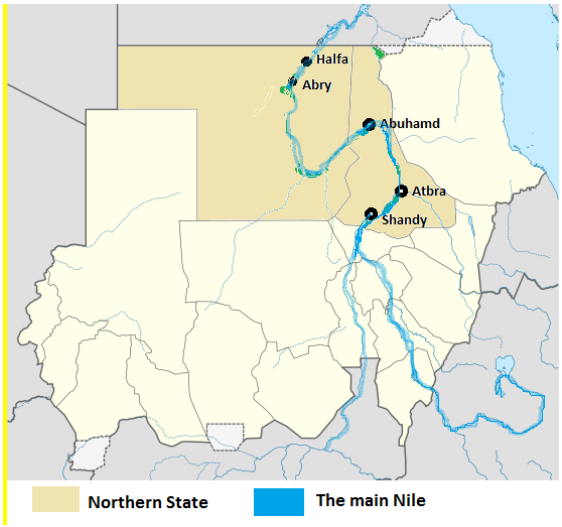

Figure 3.1 The map of areas which samples were taken from

3.3 Laser Raman Spectrometer

Laser Raman Spectrometer model Horiba Lab RAM HR 3D illustrate in figure 3.1, was used in this study to record the Raman spectra of the samples. It is power full instrument for the identification a wide range of substances in physics and chemistry laboratories. Raman spectrometer is non-destructive technique and requiring no sample preparation, and it involves illuminating a sample with monochromatic light and using spectrometer to examine the light scattered by the sample. The schematic diagram of the Horiba Lab RAM HR D3 Raman spectrometer is shown in figure (3.1).

When a light beam emitted from a laser device passes into external optic path and irradiates the sample, the scattered light enters the monochromator. When the grating in the monochromator is rotating, the spectrum message is transformed by a photomultiplier into current pulses which are enlarged and counted by photocounter and sent into computer for processing, while a spectrum curve is being displayed on a monitor. The specifications and the parameters of spectrometer are listed in table (3.1).

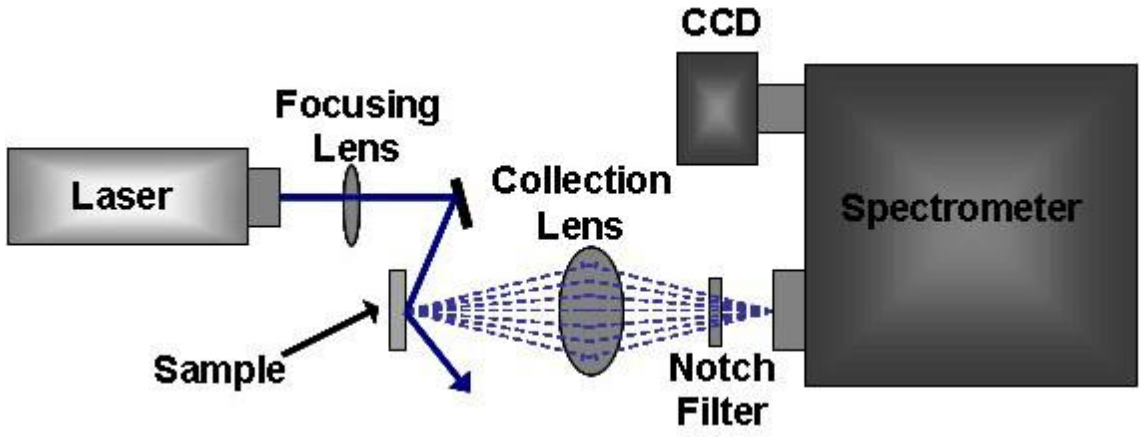

Figure 3.2 Schematic diagram of Horiba LAB RAM 3D Raman spectrometer

Table 3.1 Specifications and parameters of laser Raman Spectrometer model Horiba Lab RAM HR 3D:

Wavelength	532 nm (green)
Laser Class	Class 3B
Laser Type	Continuous wave
Max power	50 mW
Model	Ventus 532 50mW
Manufacturer	Laser Quantum

3.3.1 Laser

A diode pumped solid state green (DPSS) laser was used in the instrument as excitation light source. Its wavelength is 532 nm and it emits power up to 50 mW where its output beam is polarized one.

3.3.2 Monochromator

The optics structure of the mohnochromator is shown in figure 3.2, S1 is the entrance slit, M1is the collimating lens, and G is the diffraction grating. The diffracted beam is reflected by mirror M2 to the exit slit S2 where there is photomultiplier(PMT). When the grating is rotated, a spectrum message is transformed by the PMT into a current pulse which is enlarged and counted by photocounter and sent into the computer for processing. Then the spectrum distribution curve is displayed on the screen of the monitor. The best imaging position can be found by observing intensity of some Raman lines scanned by the monochromator.

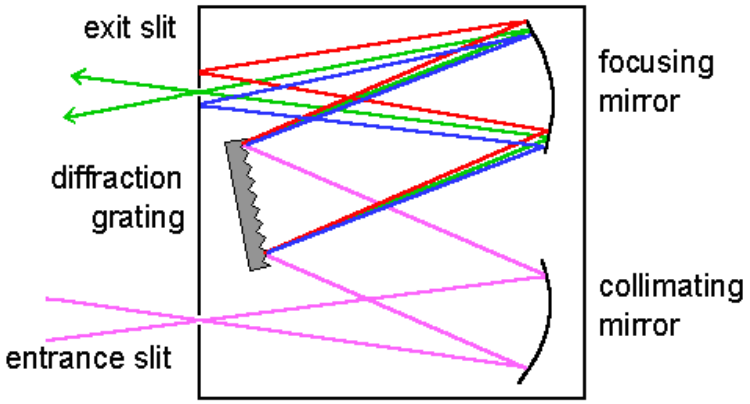

Figure 3.3 The Monochromatic

3.3.3 Charge Coupled Devices (CCDs)

The CCDs consist of a large matrix of pixel elements, the fundamental structure of which is a metal-oxide-semiconductor diode on a thin silicon substrate (Hardy, T.D.; 1998). A polysilicon gate is deposited on top of each pixel, and an external bias is applied to the gate to control the potential of the region beneath the gate. By applying different biases (reverse bias and zero), an individual pixel is isolated from the neighboring pixels because of the insulating barriers (potential well shown in Figure 5). For pixels that are reverse-biased, depletion regions are formed, and charges are held and stored within the potential well up to the full well when illumination is applied. In contrast, those zero-biased pixels are

transparent to the incoming photons. The number of charges generated is proportional to the intensity of the incident light flux, and the full well capacity determines the maximum light intensity that can be detected. By adjusting the bias, carriers stored in the potential well can be transferred to the output of the detector (Hardy, T.D.; 1999).

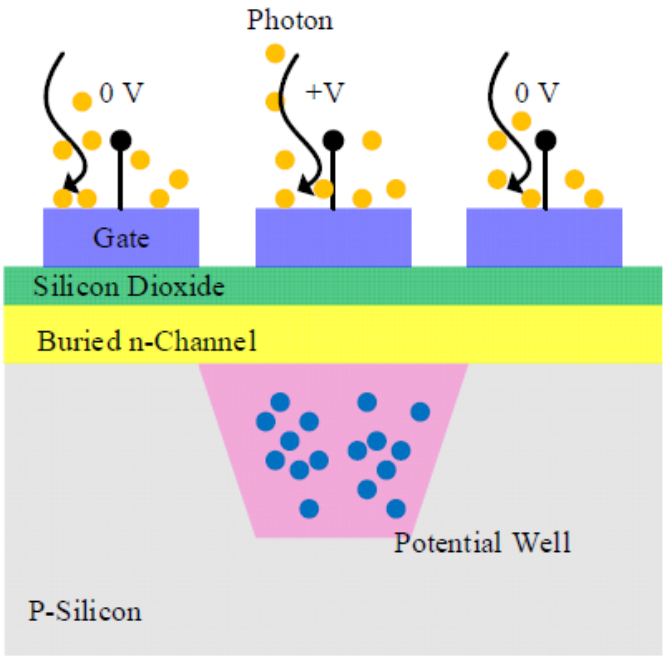

Figure 3.4 Basic structure of a charge coupled device (CCD)

3.4 Method

Figure 3.5 shows the Laser Raman Spectrometer model Horiba Lab RAM HR D3 which easy use and no sample preparation is needed. The experimental setup used in this work was arranged as shown in figure 3.6.

To run the Raman device perfectly, the work was divided to stages, carried out in order to get the best results. Reviewing the power supply and connections well, then the laser module was operated. The Raman switch was open after that. Out cover was open to see the laser path, and make it linear on all tracks, this is done in two phases, The first phase was the adjusting of the laser path vertical on the sample holder in the middle of the hole, and using the manual adjustment and simple tools (such as Cutter, ruler, paper, and gum). After making sure that the laser has become in the center of the sample holder, the second phase was started by moving the unit lenses to get a sharp line of the

laser on the region of magnification and recording signal, use screws to make adjustment, see Figure (3.3). After that the scattering laser line was centered at the hole of the magnification unit.

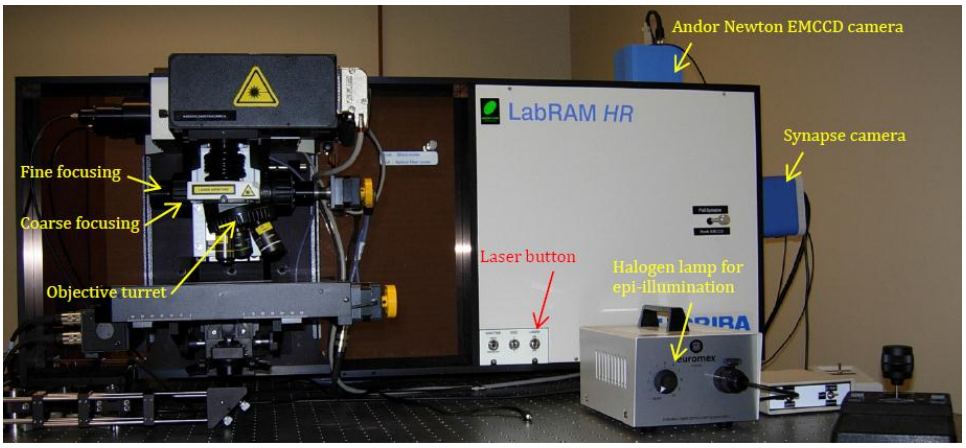

Figure 3.5 Laser Raman Spectrometer model Horiba Lab RAM HR D3

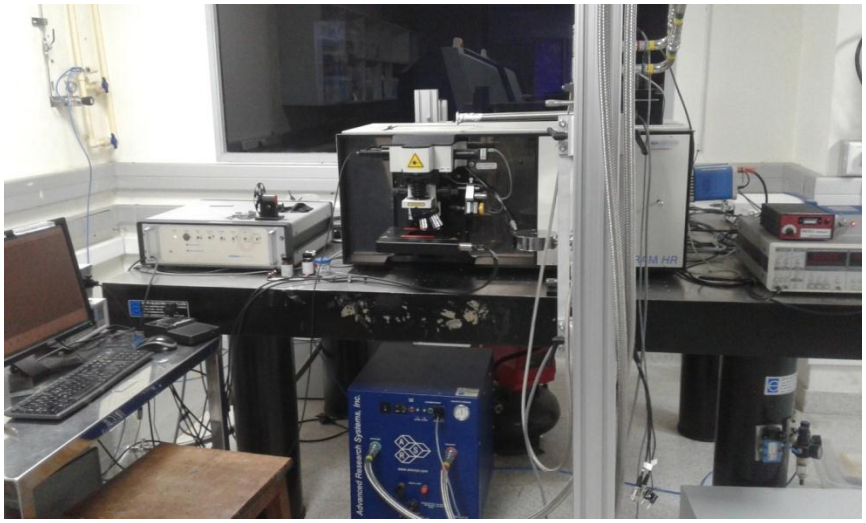

Figure 3.6 The experimental setup

Chapter Four

Results and Discussion

4.1 Introduction

The aim of this study was to mapping the molecules of water collected from some regions in the northern Sudan using Laser Raman Spectrometer model Horiba Lab RAM HR D3. The ten water samples were collected from the Nile and water lines from (Halfa, Abry, Abuhamad, Atbra and Shandy), in northern Sudan.

The results of the investigation are presented in this chapter and discussed. At end of the chapter the main conclusions and recommendation are presented.

4.2 Results and Discussion

Ten water samples were collected from the Nile and pipelines in five different areas northern Sudan. The results showed these samples contain different materials beside the water with different amounts.

The Raman spectrum of a sample taken from the Nile in the area of Halfa in the range from 389 to 2403 cm^{-1} as figure (4.1.a) shows. It shows clear peaks and by comparison with the vibrations recorded in some references, we found that these vibrations describe the vibrations of water molecules and some components of other materials as listed in Table (4.1.a).

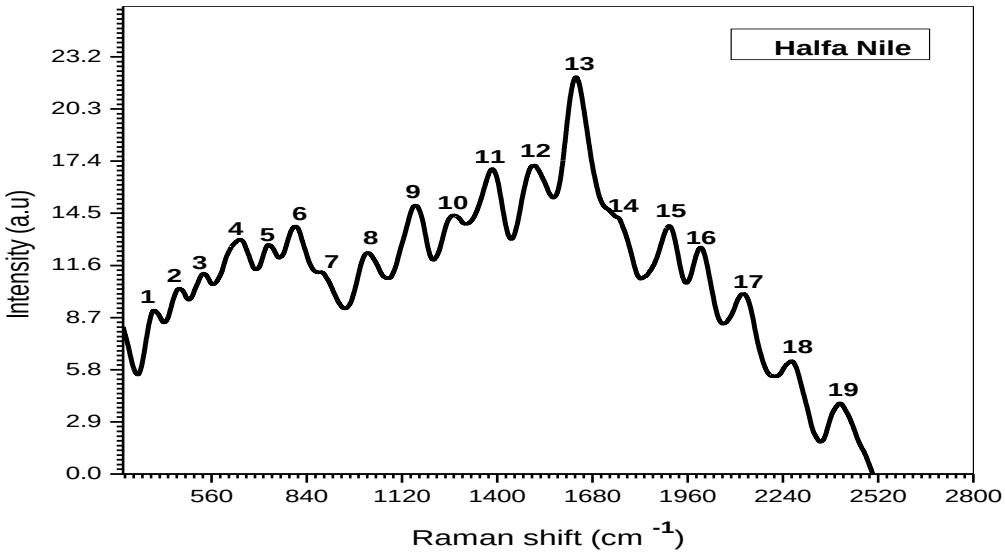

Figure 4.1.a Raman spectrum of surface water sample taken from Nile in Halfa area in the range from 389 to 2403cm^{-1}.

Table 4.1.a water sample collected from Nile in Halfa area

Peak No	Raman shift (cm^{-1})	Intensity (a.u)	Functional group	References
1	389	9.23	α Fe-OH	(Cornell, R.M. and Schwertmann, U., 2003), (Oh, S.J., Cook, D.C. and Townsend, H.E., 1998)
2	464	10.44	Si-O-Si	(Edwards HG.,2005), (Robert, M.S., et al., 2005), (MANOHARAN, R. and SETHI, N., 2003), (Socrates, G., 2004)

3	538	11.27	Si-O-Si	(Edwards HG.,2005), (Robert, M.S., et al., 2005), (MANOHARAN, R. and SETHI, N., 2003), (Socrates, G., 2004)
4	641	13.17	C=S	(Edwards HG.,2005), (Robert, M.S., et al., 2005), (MANOHARAN, R. and SETHI, N., 2003)
5	729	12.86	C-F	(Robert, M.S., et al., 2005), (Nafie A. Almusleta, et al., 2016)
6	810	13.87	ν(C-C) stretching	(De Veij, M., Vandenabeele, P., et al., 2009)
7	891.7	11.32	$UO_2{}^{+2}$antisymmetric Stretching	(Frost, R.L., et al., 2006)
8	1026	12.40	Toluene	(Li, G., Chen, M. and Wei, T., 2009)
9	1157	15.02	C–H bending	(Ćirić-Marjanović, G., et al., 2008)
10	1270	14.51	$\nu(C-N)_\beta$	(Ćirić-Marjanović, G., et al., 2008)

11	1393.6	17.11	Si – O – C	(Edwards HG.,2005), (Robert, M.S., et al., 2005),
12	1510.9	17.30	C = C	(Edwards HG.,2005), (Robert, M.S., et al., 2005), (Socrates, G., 2004), (Lin-Vien, D., et al., 1991)
13	1635	22.19	O-H bending	(Durickovic, I. and Marchetti, M., 2014)
14	1752.5	14.45	Lactone	(Edwards HG.,2005), (Robert, M.S., et al., 2005)
15	1899.4	13.94	C = C	(Edwards HG.,2005), (Robert, M.S., et al., 2005), (Socrates, G., 2004), (Lin-Vien, D., et al., 1991)
16	2000	12.73	-	-
17	2121.3	10.12	Isothiocyanate	(Edwards HG.,2005), (Robert, M.S., et al., 2005)
18	2262	6.37	Diazonium salt	(Edwards HG.,2005), (Robert, M.S., et al., 2005)

19	2403	4.02	P – H	(Edwards HG.,2005), (Robert, M.S., et al., 2005)

Figure (4.1.b) shows the Raman spectrum of a sample which taken from the water pipeline in the area of Halfa in the range from 389 to 2432cm^{-1}.Clear peaks were observed and by comparison with the vibrations recorded in previous studies and some references, we found that these vibrations describe the vibrations of water molecules and some components of other materials as listed in Table (4.1.b).

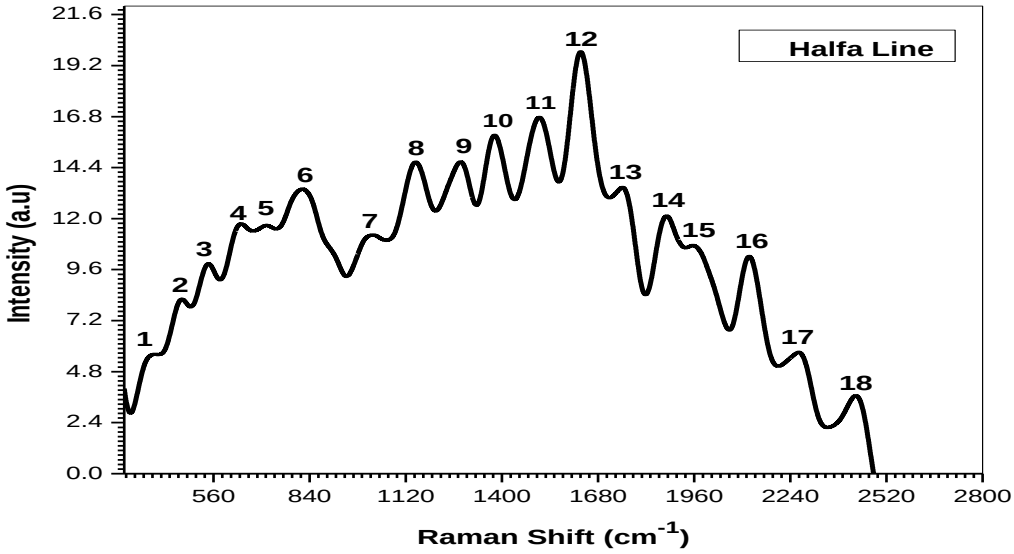

Figure 4.1.b Raman spectrum of water sample taken from pipeline in Halfa area in the range from389 to 2432cm^{-1}.

Table 4.1.b water sample collected from pipeline water in Halfa area.

Peak No	Raman shift (cm^{-1})	Intensity (a.u)	Functional group	References
1	389	5.71	α Fe-OH	(Oh, S.J., Cook, D.C. and Townsend, H.E., 1998), (Cornell, R.M. and Schwertmann, U., 2003),
2	464	8.29	Si-O-Si	(Robert, M.S., et al., 2005), (MANOHARAN, R. and SETHI, N., 2003), (Socrates, G., 2004), (Edwards HG.,2005)
3	545	9.97	Si -O- Si	(MANOHARAN, R. and SETHI, N., 2003), (Socrates, G., 2004)
4	641	11.84	C=S	(Robert, M.S., et al., 2005), (MANOHARAN, R. and SETHI, N., 2003), (Edwards HG.,2005)
5	717.2	11.79	p-xylene	(Li, G., Chen, M. and Wei, T., 2009)
6	822	13.45	$(ASO_4)^{-3}$symmetric stretching	(Frost, R.L., et al., 2006)
7	1026	11.30	Toluene	(Li, G., Chen, M. and Wei, T., 2009)
8	1152	14.75	Toluene	(Li, G., Chen, M. and Wei, T., 2009)
9	1270	14.75	$\nu(C-N)_\beta$	(Ćirić-Marjanović, G., et al., 2008)
10	1377	16.04	Toluene	(Li, G., Chen, M. and Wei, T., 2009)

11	1510.9	16.84	C = C	(Robert, M.S., et al., 2005), (Socrates, G., 2004), (Edwards HG.,2005), (Lin-Vien, D., et al., 1991)
12	1635	19.97	O-H bending	(Durickovic, I. and Marchetti, M., 2014)
13	1752.5	13.56	Lactone	(Robert, M.S., et al., 2005), (Edwards HG.,2005)
14	1877	12.23	NO	(Gang Li, Guoping Zhang, 2006)
15	1960	10.82	-	-
16	2121.3	10.34	Isothiocyanate	(Robert, M.S., et al., 2005), (Edwards HG.,2005)
17	2262	5.82	Diazonium salt	(Robert, M.S., et al., 2005), (Edwards HG.,2005)
18	2432	3.77	-	-

There are some molecules appeared in both samples from Halfa (Nile and pipeline) together which are (αFeOH, Si-O-Si, C=S, Toluene, $\nu(C-N)_{\beta}$, C=C, Lactone, Isothiocyanate and Diazonium salt). While (C-F, ν(C-C) stretching, $UO_2{}^{+2}$antisymmetric Stretching, C-H, Si – O – C and P – H) appeared in the sample collected directly from the Nile and was not appeared in the water pipeline sample. This means the water was free from these toxic molecules by the treatment plants.

Whereas the molecules such as (p-xylene, $ASO_4{}^{-3}$and NO) which appeared in the sample collected from the water pipeline sample and it were not exist in the sample collected from Nile. This refer to existence of Arsenic and Nitrate elements in water components after the purification process and before the flow of water in the

transmission pipelines (see table 4.6). This indicates the weakness of the efficiency and the work of purification plants in the Halfa area.

Figure (4.2.a) shows the Raman spectrum in the range from 464 to 2858.2 cm^{-1} of a surface water sample taken from Nile in the area of Abry. clear peaks describe the vibration of water molecules and some components to other materials as illustrated in Table (4.2.a).

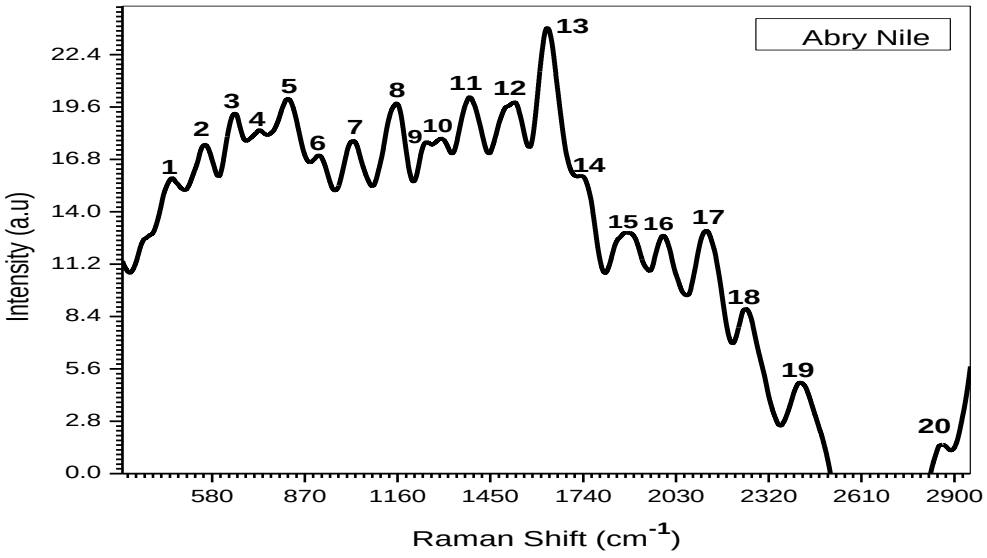

Figure 4.2.a Raman spectrum of surface water sample taken from Nile in Abry area in the range from 464 to 2858.2 cm^{-1}.

Table 4.2.a water sample collected from Nile in Abry area

Peak No	Raman shift (cm^{-1})	Intensity (a.u)	Functional group	References
1	464	15.90	Si-O-Si	(Edwards HG.,2005), (Robert, M.S., et al., 2005), (MANOHARAN, R. and SETHI, N., 2003), (Socrates, G., 2004)
2	560	17.68	α Fe-OH	(Cornell, R.M. and Schwertmann, U., 2003), (Oh, S.J., Cook, D.C. and Townsend, H.E., 1998)
3	650	19.33	FeII-O	Nafie A. Almusleta, et al., 2016)
4	729	18.47	C-F	(Robert, M.S., et al., 2005), (Nafie A. Almusleta, et al., 2016)
5	810	20.12	ν(C–C) stretching	(De Veij, M., Vandenabeele, P., et al., 2009)
6	910	17.31	Aromatic C–H	(Durickovic, I. and Marchetti, M., 2014)
7	1026	17.92	Toluene	(Li, G., Chen, M. and Wei, T., 2009)
8	1152	19.93	Toluene	(Li, G., Chen, M. and Wei, T., 2009)

9	1257	17.86	C–O	(Durickovic, I. and Marchetti, M., 2014)
10	1285	18.05	CO stretch and strong ring-H and COH rocking motions	(Fangyuan Han, Weimin Liu and Chong Fang, 2013)
11	1393.6	20.25	Si – O – C	(Edwards HG.,2005), (Robert, M.S., et al., 2005)
12	1522.9	20.00	C = C	(Edwards HG.,2005), (Robert, M.S., et al., 2005), (Socrates, G., 2004), (Lin-Vien, D., et al., 1991)
13	1635	23.90	O-H bending	(Durickovic, I. and Marchetti, M., 2014)
14	1732.1	16.02	Ester	(Edwards HG.,2005), (Robert, M.S., et al., 2005)
15	1876	13.03	C=O stretching	(Phongpa-Ngan, P., et al., 2014)
16	1991	12.84	-	-
17	2130.3	13.03	Isothiocyanate	(Edwards HG.,2005), (Robert, M.S., et al., 2005)
18	2239	8.93	C≡N stretch	(Ito, K., Kato, T. and Ona, T., 2002)

19	2422	4.96	-	-
20	2858.2	1.67	C – CH3	(Edwards HG.,2005), (Robert, M.S., et al., 2005)

The Raman spectrum of a sample which taken from the water treatment plant in the area of Abry in the range from 481 to 2436 cm^{-1} as shown in figure (4.2.b) beside the vibrations of water molecules some other vibrations were appeared in the spectrum. As shown in Table (4.2.b).

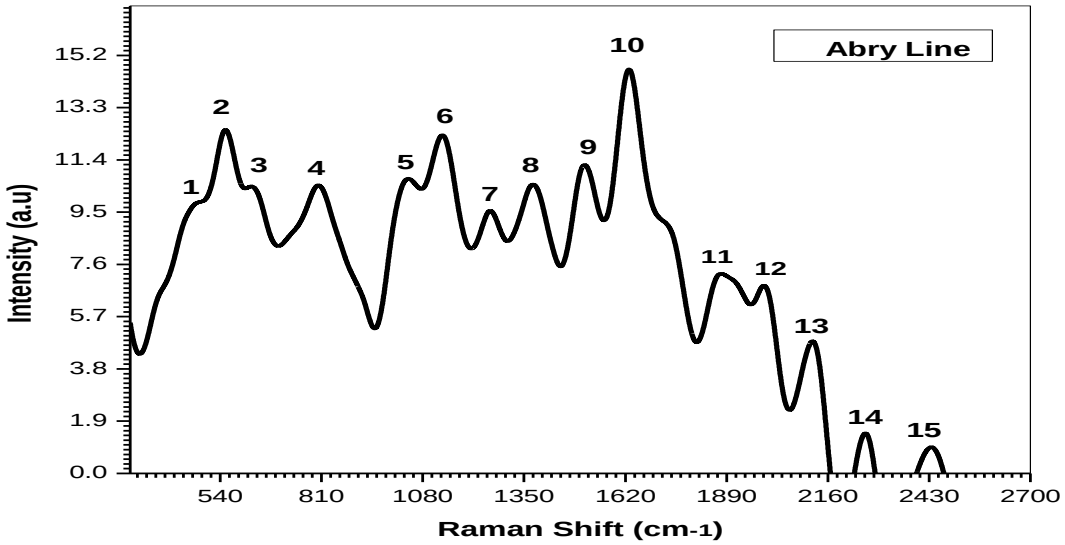

Figure 4.2.b Raman spectrum of water sample taken from pipeline in Abry area in the range from 481 to 2436cm^{-1}.

Table 4.2.b water sample collected from pipeline in Abry area

Peak No	Raman shift (cm^{-1})	Intensity (a.u)	Functional group	References
1	481	9.94	-	-
2	545	12.56	Si -O- Si	(MANOHARAN, R. and SETHI, N., 2003), (Socrates, G., 2004)
3	625.1	10.48	C = S	(Robert, M.S., et al., 2005), (Edwards HG.,2005)
4	810	10.56	*v*(C-C) stretching vibration	(De Veij, M., Vandenabeele, P., et al., 2009)
5	1041.3	10.81	Sulfonic acid	(Robert, M.S., et al., 2005), (Edwards HG.,2005)
6	1136	12.39	ν_3 symmetric stretching of the perchlorate ion	(Sobrón, P., et al., 2007)
7	1257	9.61	C-O	(Durickovic, I. and Marchetti, M., 2014)
8	1374.1	10.56	Ethylbenzene	(Li, G., Chen, M. and Wei, T., 2009)

9	1510.9	11.27	C = C	(Robert, M.S., et al., 2005), (Socrates, G., 2004), (Edwards HG.,2005), (Lin-Vien, D., et al., 1991)
10	1635	14.76	O-H bending	(Durickovic, I. and Marchetti, M., 2014)
11	1877	7.32	NO	(Gang Li, Guoping Zhang, 2006)
12	1988	6.91	-	-
13	2121.3	4.87	Isothiocyanate	(Robert, M.S., et al., 2005), (Edwards HG.,2005)
14	2262	1.55	Diazonium salt	(Robert, M.S., et al., 2005), (Edwards HG.,2005)
15	2436	1.00	-	-

The molecules such as (Si-O-Si, ν(C-C, C-O, C=C and O-H bending) were observed in both Nile and pipeline water samples collected from Abry area. And (α Fe-OH, FeII-O, C-F, Aromatic C–H, Toluene, CO stretch, Si – O – C, Ester, C=O, Thiocyanate, C≡N stretch and C – CH3) molecules were found in the sample collected directly from the Nile and were not found in the water pipeline sample. This means the water was purified by the treatment plants from trace molecules such as (C≡N and Toluene). Whereas molecules such as (C=S, Sulfonic acid, perchlorate, Ethylbenzene, NO, Isothiocyanate and Diazonium salt) appeared in

the sample collected from the water pipeline sample and it were not exist in the sample collected from Nile. These molecules were formed as a result of interactions between water purification additives, some chemical compounds such as calcium hydroxide and sodium carbonate are added for precipitation and Aluminum sulfate for Coagulation (note that, existence of Sulfate and Nitrate elements in water components after the purification process and before the flow of water in the transmission pipelines (see table 4.6)). As well as the result of pollution of water while running in the transmission lines.

The water sample which taken from the Nile in Abuhamad area, clear picture of the water components and some other materials as in figure (4.3.a) and Table (4.3.a) illustrates the analysis of this spectrum.

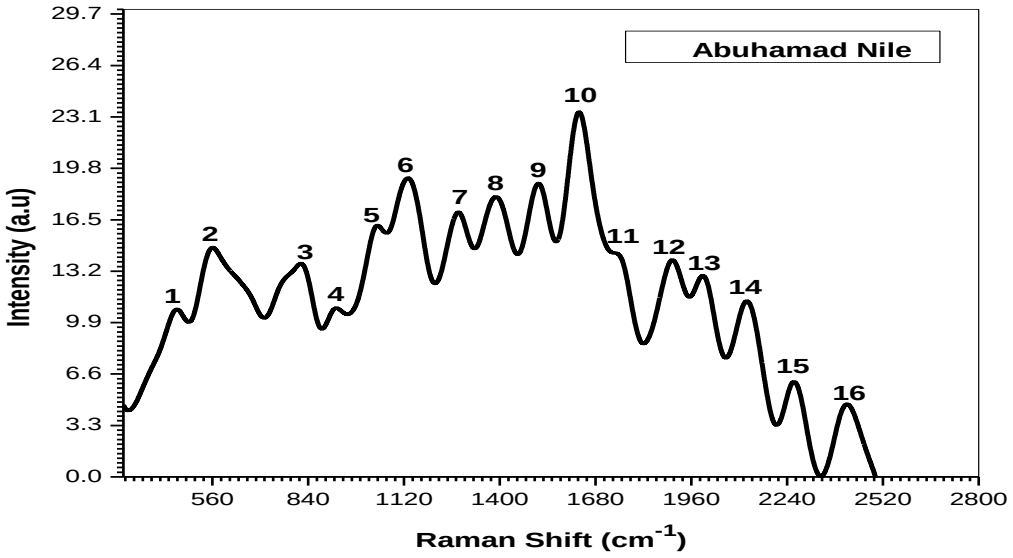

Fig 4.3.a Raman spectrum of water sample taken from Nile in Abuhamad area in the range from 464 to 2411.6 cm^{-1}.

Table 4.3.a water sample collected from Nile in Abuhamad area

Peak No	Raman shift (cm^{-1})	Intensity (a.u)	Functional group	References
1	464	10.87	Si-O-Si	(Edwards HG.,2005), (Robert, M.S., et al., 2005), (MANOHARAN, R. and SETHI, N., 2003), (Socrates, G., 2004)
2	560	14.48	αFe-OH	(Cornell, R.M. and Schwertmann, U., 2003), (Oh, S.J., Cook, D.C. and Townsend, H.E., 1998)
3	822	13.80	$(ASO_4)^{-3}$symmetric stretching	(Frost, R.L., et al., 2006)
4	936	10.95	$PO_4{}^{-3}$	(Mabrouk, K.B., et al., 2013)
5	1041.3	16.30	Sulfonic acid	(Edwards HG.,2005), (Robert, M.S., et al., 2005),
6	1136	19.31	ν_3 symmetric stretching of the perchlorate ion	(Sobrón, P., et al., 2007)
7	1270	17.10	$\nu(C-N)_\beta$	(Ćirić-Marjanović, G., et al., 2008)

8	1393.6	18.13	Si – O – C	(Edwards HG.,2005), (Robert, M.S., et al., 2005),
9	1510.9	18.93	C = C	(Edwards HG.,2005), (Robert, M.S., et al., 2005), (Socrates, G., 2004), (Lin-Vien, D., et al., 1991)
10	1635	23.56	O-H bending	(Durickovic, I. and Marchetti, M., 2014)
11	1752.5	14.46	Lactone	(Edwards HG.,2005), (Robert, M.S., et al., 2005),
12	1899.4	14.02	C = C	(Edwards HG.,2005), (Robert, M.S., et al., 2005), (Socrates, G., 2004), (Lin-Vien, D., et al., 1991)
13	1994	13.00	-	-
14	2121.3	11.38	Isothiocyanate	(Edwards HG.,2005), (Robert, M.S., et al., 2005),
15	2262	6.25	Diazonium salt	(Edwards HG.,2005), (Robert, M.S., et al., 2005),

16	2411.6	4.79	P – H	(Edwards HG.,2005), (Robert, M.S., et al., 2005),

Figure (4.3.b) shows the Raman spectrum of a sample which taken from the water treatment plant in the area of Abohamd in the range from 456 to 2630 cm^{-1}.Clear peaks were observed and by comparison with the vibrations recorded in previous studies and some references, we found that these vibrations describe the vibrations of water molecules and some components of other materials as listed in Table (4.3.b).

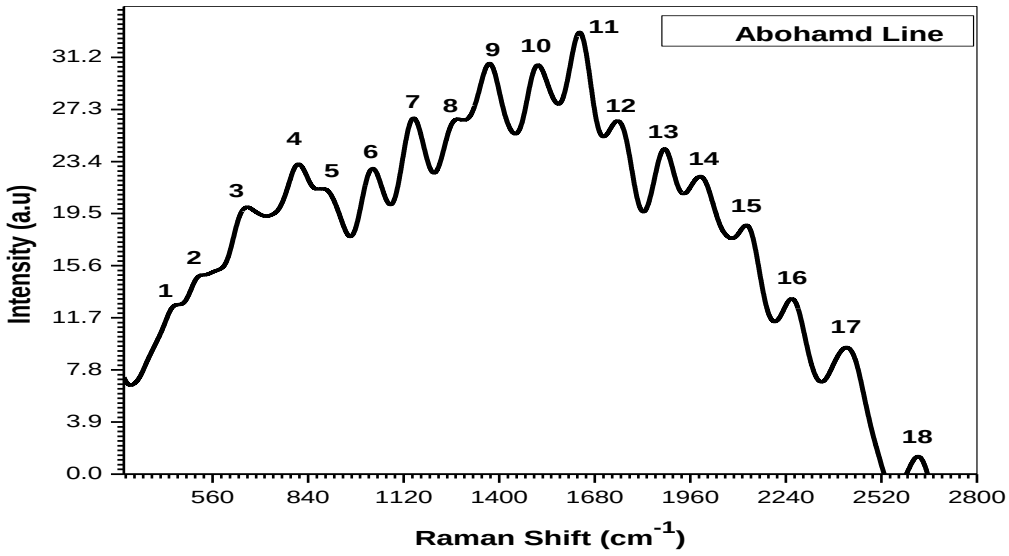

Figure 4.3.b Raman spectrum of water sample taken from pipeline in Abohamd area in the range from 456 to 2630 cm^{-1}.

Table 4.3.b water sample collected from pipeline in Abohamd area

Peak No	Raman shift(cm^{-1})	Intensity(a.u)	Functional group	References
1	456	12.85	Si-O-Si	(Ferraro, J.R., et al., 2003), (Robert, M.S., et al., 2005), (MANOHARAN, R. and SETHI, N., 2003), (Socrates, G., 2004),
2	538	15.07	Si-O-Si	(Robert, M.S., et al., 2005), (MANOHARAN, R. and SETHI, N., 2003), (Socrates, G., 2004), (Edwards HG.,2005)
3	660	20.12	FeIII-O	(Oh, S.J., Cook, D.C. and Townsend, H.E., 1998)
4	810	23.37	*v*(C-C) stretching vibration	(De Veij, M., Vandenabeele, P., et al., 2009)
5	891.7	21.50	UO_2^{+2} antisymmetric Stretching	(Frost, R.L., et al., 2006)
6	1030	23.03	δ (C–H) δ: bending mode	(Başar, G., et al., 2012)
7	1152	26.80	Toluene	(Li, G., Chen, M. and Wei, T., 2009)

8	1270	26.72	$\nu(C-N)_{\beta}$	(Ćirić-Marjanović, G., et al., 2008)
9	1374.1	30.91	Ethylbenzene	(Li, G., Chen, M. and Wei, T., 2009)
10	1510.9	30.83	C = C	(Robert, M.S., et al., 2005), (Socrates, G., 2004), (Socrates, G., 2004), (Edwards HG.,2005)7,9,14,15
11	1635	33.22	O-H bending	(Durickovic, I. and Marchetti, M., 2014)
12	1752	26.55	Lactone	(Robert, M.S., et al., 2005), (Edwards HG.,2005)
13	1876	24.48	C=O stretching	(Phongpa-Ngan, P., et al., 2014)
14	1990	22.43	-	-
15	2121.3	18.76	Isothiocyanate	(Robert, M.S., et al., 2005), (Edwards HG.,2005)
16	2262	13.27	Diazonium salt	(Robert, M.S., et al., 2005), (Edwards HG.,2005)
17	2411.6	9.60	P – H	(Robert, M.S., et al., 2005), (Edwards HG.,2005)
18	2630	1.47	-	-

(Si-O-Si, $\nu(C-N)_{\beta}$, C=C, O-H bending, Lactone, Isothiocyanate, Diazonium salt and P – H) molecules appeared in both samples from Halfa (Nile and pipeline) together. While molecules such as (αFe-OH, $(ASO_4)^{-3}$,

PO_4^{-3} , Sulfonic acid, perchlorate and Si – O – C) appeared in the sample collected directly from the Nile and was not appeared in the water pipeline sample. This means the water was free from these toxic molecules ($(ASO_4)^{-3}$, PO_4^{-3}) by the treatment plants.

Whereas the molecules such as (FeIII-O, $\nu(C-C)$, UO_2^{+2}, C–H, Toluene, Ethylbenzen and C=O) which appeared in the sample collected from the water pipeline sample and it were not exist in the sample collected from Nile. and this refer to pollution of the water while running in the transmission lines as well as result of adding sand for sedimentation. (note that, existence of Uranium elements and Ethylbenzen in water components after the purification process and before the flow of water in the transmission pipelines (see table 4.6)).

The continued appearance of ($\nu(C-N)_\beta$ and P – H) molecules in water samples after purification is evidence that the purification has not been fully operational.

Figure (4.4.a) shows the Raman spectrum of the sample collected from the Nile in the Atbra area. beside the vibrations of water molecules some other vibrations were appeared in the spectrum. As shown in Table (4.4.a).

Figure 4.4.a Raman spectrum of water sample taken from Nile in Atbra area in the range from 421 to 2875cm^{-1}.

Table 4.4.a water sample collected from Nile Atbra area

Peak No	Raman shift (cm^{-1})	Intensity (a.u)	Functional group	References
1	421	7.88	C–N–C	(Sobrón, P., et al., 2007)
2	538	9.60	Si-O-Si	(Edwards HG.,2005), (Robert, M.S., et al., 2005), (MANOHARAN, R. and SETHI, N., 2003), (Socrates, G., 2004)
3	670	10.62	βFe-OH	(Shebanova, O.N. and Lazor, P., 2003)
4	764	11.02	C-F	(Edwards HG.,2005), (Robert, M.S., et al., 2005)

5	822	11.49	$(ASO_4)^{-3}$symmetric stretching	(Frost, R.L., et al., 2006)
6	1026	8.71	Toluene	(Li, G., Chen, M. and Wei, T., 2009)
7	1136	11.02	ν_3 symmetric stretching of the perchlorate ion	(Sobrón, P., et al., 2007)
8	1285	11.20	CO stretch and strong ring-H and COH rocking motions	(Fangyuan Han, Weimin Liu and Chong Fang, 2013)
9	1374	11.89	Ethylbenzene	(Li, G., Chen, M. and Wei, T., 2009)
10	1510.9	12.92	C = C	Edwards HG.,2005), (Robert, M.S., et al., 2005), (Socrates, G., 2004), (Lin-Vien, D., et al., 1991)
11	1635	17.86	O-H bending	(Durickovic, I. and Marchetti, M., 2014)
12	1876	8.57	C=O stretching	(Phongpa-Ngan, P., et al., 2014)
13	1970	8.42	-	-
14	2106	7.15	-	-

15	2239	4.48	C≡N stretch	(Ito, K., Kato, T. and Ona, T., 2002)
16	2411.6	2.99	P – H	(Edwards HG.,2005), (Robert, M.S., et al., 2005)
17	2875	1.38	-	-

Figure (4.4.b) illustrates Raman spectrum of the water collected from the water treatment plant in the area of Atbra in the range from 389 to 2403 cm^{-1}. Table (4..4.b) lists the analysis of this spectrum.

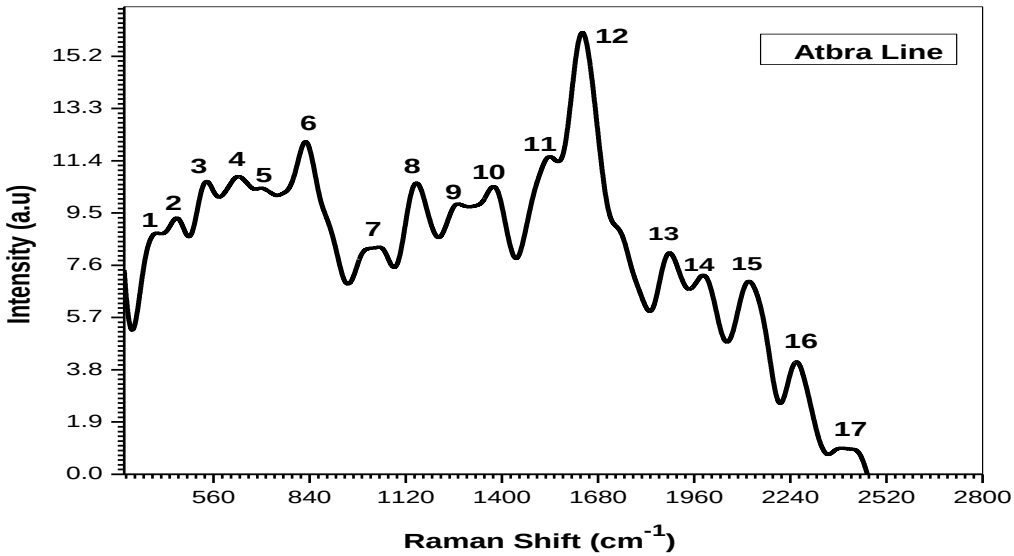

Figure 4.4.b Raman spectrum of water sample taken from pipeline in Atbra area in the range from 389 to 2403 cm^{-1}.

Table 4.4.b water sample collected from pipeline Atbra area

Peak No	Raman shift (cm^{-1})	Intensity (a.u)	Functional group	References
1	389	8.86	α Fe-OH	Oh, S.J., Cook, D.C. and Townsend, H.E., 1998), (Cornell, R.M. and Schwertmann, U., 2003),
2	456	9.40	Si-O-Si	(Robert, M.S., et al., 2005), (MANOHARAN, R. and SETHI, N., 2003), (Socrates, G., 2004)
3	538	9.60	Si-O-Si	(Ferraro, J.R., et al., 2003), (Robert, M.S., et al., 2005), (MANOHARAN, R. and SETHI, N., 2003), (Socrates, G., 2004), (Edwards HG.,2005)
4	635	10.90	Acetylene C–H bending	(X. Song et al., 2013)
5	704	10.48	CaCO3	(Seok Chan Park, Minjung Kim and et al., 2009)
6	840	12.19	As–O asymmetric vibration	X. Song et al., 2013

7	1030	8.32	δ (C–H) δ: bending mode	(Khetan, S.K. and Collins, T.J., 2007)
8	1152	10.65	Toluene	(Li, G., Chen, M. and Wei, T., 2009)
9	1270	9.90	$\nu(C-N)_{\beta}$	(Ćirić-Marjanović, G., et al., 2008)
10	1377	10.53	Toluene	(Li, G., Chen, M. and Wei, T., 2009)
11	1535	11.60	amide II	(Phongpa-Ngan, P., et al., 2014)
12	1635	16.14	O-H bending	(Durickovic, I. and Marchetti, M., 2014)
13	1899.4	8.11	C = C	(Robert, M.S., et al., 2005), (Socrates, G., 2004), (Edwards HG.,2005), (Lin-Vien, D., et al., 1991)
14	1984	7.32	-	-
15	2121.3	7.08	Isothiocyanate	(Robert, M.S., et al., 2005), (Edwards HG.,2005)
16	2262	4.16	Diazonium salt	(Robert, M.S., et al., 2005), (Edwards HG.,2005)
17	2403	1.05	P – H	(Robert, M.S., et al., 2005), (Edwards HG.,2005)

Some molecules appeared in both samples from Atbra (Nile and pipeline) together which were (Si-O-Si, αFeOH, Toluene, C=C, O-H bending and P – H). While

(C–N–C, C-F, $(ASO_4)^{-3}$, perchlorate, CO stretch, Ethylbenzene, C=O stretching and C≡N stretch) appeared in the sample collected directly from the Nile and did not appear in the water pipeline sample. This means the water was free from these toxic molecules ($(ASO_4)^{-3}$, Ethylbenzene and C≡N) by the treatment plants. Whereas the molecules such as (C–H, CaCO3, As–O, $\nu(C-N)_\beta$ amide II, Isothiocyanate and Diazonium salt) appeared in the sample collected from the water pipeline sample and it was not exist in the sample collected from Nile. And this refer to pollution of the water while running in the transmission lines and also due to interactions between water purification additives, some chemical compounds such as calcium hydroxide and sodium carbonate are added for precipitation and Aluminum sulphate for Coagulation. (note that, existence of Cyanide and Acrylamide elements in water components after the purification process and before the flow of water in the transmission pipelines (see table 4.6)).

Also the appearance of (Toluene and P – H) even after the purification process indicates that, water has not been purified as it should.

Figure (4.5.a) illustrates Raman spectrum of the water collected from the Nile in area of Shandy in the range from 464 to 2411.6 cm^{-1}. Table (4.5.a) lists the analysis of this spectrum.

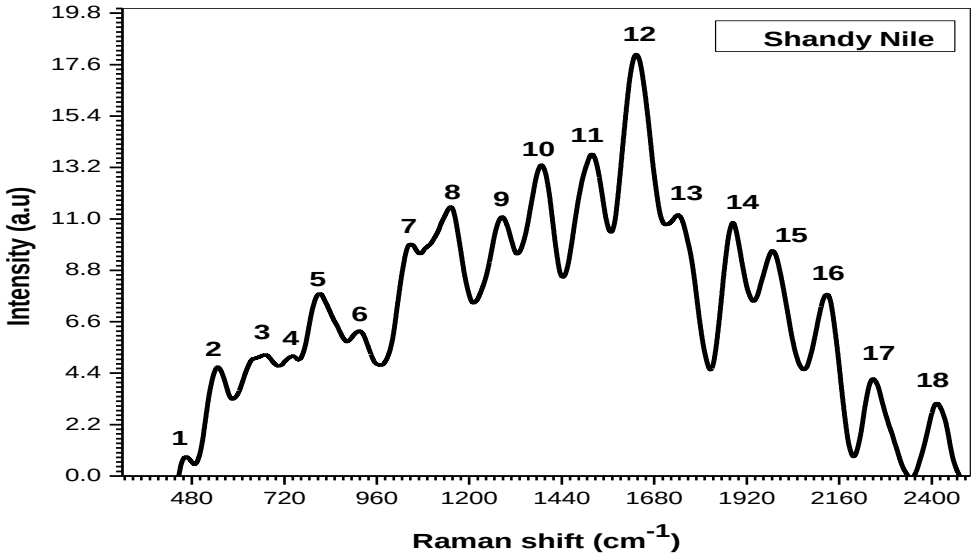

Figure 4.5.a Raman spectrum of water sample taken from Nile in Shandy area in the range from 464 to 2411.6cm^{-1}.

Table 4.5.a water sample collected from Nile in Shandy area

Peak No	Raman shift (cm^{-1})	Intensity (a.u)	Functional group	References
1	464	0.90	Si-O-Si	Edwards HG.,2005), (Robert, M.S., et al., 2005), (MANOHARAN, R. and SETHI, N., 2003), (Socrates, G., 2004)
2	545	4.75	Si -O- Si	(MANOHARAN, R. and SETHI, N., 2003), (Socrates, G., 2004)
3	670	5.29	βFe-OH	Shebanova, O.N. and Lazor, P., 2003)

4	741	5.25	-	-
5	810	7.88	ν(C-C) stretching	(De Veij, M., Vandenabeele, P., et al., 2009)
6	910	6.32	Aromatic C-H	(Durickovic, I. and Marchetti, M., 2014)
7	1052	9.99	NO^{-3}	(Durickovic, I. and Marchetti, M., 2014)
8	1152	11.60	Toluene	(Li, G., Chen, M. and Wei, T., 2009)
9	1285	11.16	CO stretch and strong ring-H and COH rocking motions	(Fangyuan Han, Weimin Liu and Chong Fang, 2013)
10	1393.6	13.41	Si – O – C	(Edwards HG.,2005), (Robert, M.S., et al., 2005)
11	1516.9	13.85	C = C	(Edwards HG.,2005), (Robert, M.S., et al., 2005), (Socrates, G., 2004), (Lin-Vien, D., et al., 1991)
12	1635	18.10	O-H bending	(Durickovic, I. and Marchetti, M., 2014)
13	1752.5	11.26	Lactone	(Edwards HG.,2005), (Robert, M.S., et al., 2005)
14	1886	10.92	C=O stretching	(Phongpa-Ngan, P., et al., 2014)

15	1987	9.74	-	-
16	2130.3	7.84	Thiocyanate	(Edwards HG.,2005), (Robert, M.S., et al., 2005)
17	2239	4.22	C≡N stretch	(Ito, K., Kato, T. and Ona, T., 2002)
18	2411.6	3.19	P – H	(Edwards HG.,2005), (Robert, M.S., et al., 2005)

Figure (4.5.b) illustrates Raman spectrum of the a sample which collected from the water treatment plant in the area of area of Shandy in the range from 389 to 2411.6 cm^{-1}. Table (4.5.b) lists the analysis of this spectrum.

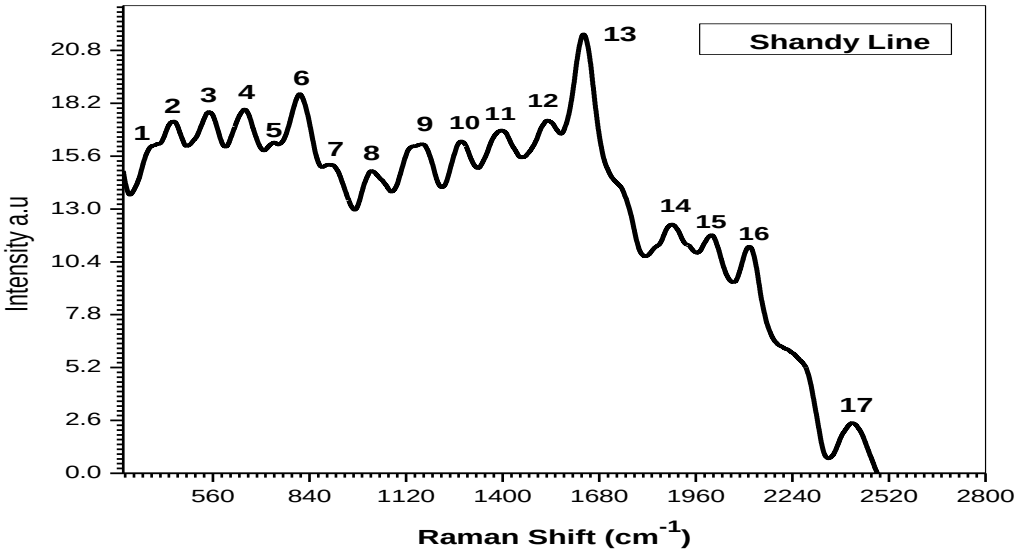

Figure 4.5.b Raman spectrum of water sample taken from pipeline in Shandy area in the range from 389 to 2411.6cm^{-1}.

Table 4.5.b water sample collected from pipeline Shandy area

Peak No	Ramanshift cm^{-1}	Intensity(a.u)	Functional group	References
1	389	16.26	α Fe-OH	(Oh, S.J., Cook, D.C. and Townsend, H.E., 1998), (Cornell, R.M. and Schwertmann, U., 2003),
2	448	17.44	S-S	(Robert, M.S., et al., 2005), (MANOHARAN, R. and SETHI, N., 2003), (Socrates, G., 2004), (Edwards HG.,2005)
3	545	17.90	Si -O- Si	(MANOHARAN, R. and SETHI, N., 2003), (Socrates, G., 2004)
4	650	18.01	FeII-O	(Nafie A. Almusleta, et al., 2016)
5	737	16.38	-	-
6	810	18.74	*v*(C-C) stretching vibration	(De Veij, M., Vandenabeele, P., et al., 2009)
7	891.7	15.31	UO_2^{+2} antisymmetric Stretching	(Frost, R.L., et al., 2006)
8	1026	14.97	Toluene	(Li, G., Chen, M. and Wei, T., 2009)

9	1152	16.31	Toluene	(Li, G., Chen, M. and Wei, T., 2009)
10	1270	16.43	$\nu(C-N)_{\beta}$	(Ćirić-Marjanović, G., et al., 2008)
11	1396.6	16.94	Aromatic azo	(Robert, M.S., et al., 2005), (Edwards HG.,2005)
12	1535	17.44	amide II	(Phongpa-Ngan, P., et al., 2014)
13	1635	21.72	O-H bending	(Durickovic, I. and Marchetti, M., 2014)
14	1890	12.33	-	-
15	2004	11.81	-	-
16	2121.3	11.26	Isothiocyanate	(Robert, M.S., et al., 2005), (Edwards HG.,2005)
17	2221.5	6.20	Aromatic nitrile	
18	2411.6	2.60	P – H	(Robert, M.S., et al., 2005), (Edwards HG.,2005)

(Si-O-Si, αFeOH, ν(C-C), Toluene, O-H bending and P – H) molecules appeared in both samples from Shandy (Nile and pipeline) together. While (Aromatic C-H, NO^{-3}, CO, Si – O – C, C = C, Lactone, C=O stretching, Thiocyanate and C≡N stretch) appeared in the sample collected directly from the Nile and were not appeared in the water pipeline sample. This means the water was free from these toxic molecules (NO^{-3} and C≡N) by the treatment plants.

Whereas the molecules such as (S-S, $UO_2{}^{+2}$, $\nu(C-N)$, Aromatic azo, amide II, Isothiocyanate and Aromatic nitrile) which appeared in the sample collected from the water pipeline sample and it were not exist in the sample collected from Nile. This refer to pollution of the water while running in the transmission lines. And also as the result of interactions between water purification additives, some chemical compounds such as calcium hydroxide and sodium carbonate are added for precipitation and Aluminum sulphate for Coagulation and Carbon dioxide as an antiseptic to kill undesirable small organisms in water. And adding sand for sedimentation. (note that, existence of Cyanide, Acrylamide Uranium and Nitrate elements in water components after the purification process and before the flow of water in the transmission pipelines (see table 4.6)).

Also the appearance of (Toluene and P – H) even after the purification process indicates that, water has not been purified as it should.

Table 4.6 Water components after the purification process and before the flow of water in the transmission pipelines in five areas

Iron
Arsenic
Lactone
Nitrate
Magnesium
Ethylbenzene
Isotl
Acrylamide
Chlorite
Isothiocyanate
Sodium
Sulfate
Sulfonic Asid
Xylenes
Diazonium Salt

Zinc
Uranium
Cyanide
Toluene
Chlorate
Nickel
$Caco_3$
Amide

4.3 Conclusion

Raman Spectroscopy is one of the best techniques that can be used to identify the surface water components. And It provides precise information about other materials found in the samples. The Raman spectra intensity of molecules is directly proportional to its concentration. It is very easy to quantitatively calculate the molar concentrations of components in water.

After the study, the water was found contain (O-H bending, α Fe-OH, Si-O-S, C=S, C-F, ν(C-C) stretching, Toluene, C–H bending, p-xylene, P – H, Lactone, C=C, Si – O – C, NO, Isothiocyanat, Diazonium salt, FeII-O, C–O, $(ASO_4)^{-3}$, Ester, C=O, C≡N stretch, $UO_2{}^{+2}$, C–N–C, $\nu(C-N)_\beta$, NO, Aromatic azo, Amide II, Aromatic nitrile, $CaCO_3$, As–O, Ethylbenzene, Sulfonic acid, FeIII-O, $PO_4{}^{-3}$, C– CH_3 and Thiocyanate, S-S, C–H, perchlorate and NO^{-3}) molecules.

The results and the study show the low quality of water in northern Sudan because it contains many of the toxic compounds Such as ($\nu(C-N)_\beta$and P – H) , (S-S, $UO_2{}^{+2}$, $(ASO_4)^{-3}$and NO).

4.4 Recommendations

The results and the study show the low quality of water in northern Sudan because it contains many of the toxic compounds. Accordingly, we recommend the Government of Sudan and the Ministry of Water and Irrigation in Sudan to improve the work and efficiency of drinking water treatment plants in Northern Sudan, as well as increase the number of water treatment plants.

It is also recommended that further studies be carried out to characterize surface and groundwater for all parts of the Sudan east, west, south and the middle.

References

Townes, C.H. and Schawlow, A.L., 2013. Microwave spectroscopy. Courier Corporation.

Wang, Z.G. and Xia, H.R., 2012. Molecular and laser spectroscopy (Vol. 50). Springer Science & Business Media.

Huber, K.P., 2013. Molecular spectra and molecular structure: IV. Constants of diatomic molecules. Springer Science & Business Media.

Landau, L.D. and Lifshitz, E.M., 2013. Quantum mechanics: non-relativistic theory (Vol. 3). Elsevier.

Atkins, P.W., Paula J de 2006 Physical Chemistry.

Baer, B.J., Evans, W.J. and Yoo, C.S., 2007. Coherent anti-stokes Raman spectroscopy of highly compressed solid deuterium at 300 K: Evidence for a new phase and implications for the band gap. Physical review letters, 98(23), p.235503.

Wright, A.J. and Lee, M.R., 2012. THE USE OF RAMAN SPECTROSCOPY TO CHARACTERIZE BIOLOGICAL AND BIOMINERALIC CRUSTS.

Durickovic, I. and Marchetti, M., 2014. Raman spectroscopy as polyvalent alternative for water pollution detection. IET Science, Measurement & Technology, 8(3), pp.122-128.

Bumbrah, G.S. and Sharma, R.M., 2016. Raman spectroscopy–Basic principle, instrumentation and selected applications for the characterization of drugs of abuse. Egyptian Journal of Forensic Sciences, 6(3), pp.209-215.

Nafie A. Almuslet and Mohammed A. Yousif, 2016. Identification of Groundwater Components In Western Part Of Saudi Arabia Using Raman Spectroscopy, Journal of Multidisciplinary Engineering Science and Technology (JMEST) ISSN: 2458-9403 Vol. 3 Issue 4.

Nafie A. Almuslet, Mubarak M. Ahmed and Siham M. Hassen, 2017. Usage of Laser Raman spectroscopy to identify the unstable compounds of iron oxides.

Mukhopadhyay, A. and Dubey, P., 2018. Investigation of solvation of ammonium salts: A Raman spectroscopy and ab initio study. Journal of Raman Spectroscopy, 49(4), pp.736-746.

DV and as, S.J., Winter, T.C. and Battaglin, W.A., 2002. Water and the Environment. American Geological Institute.

Melissa Valentine, et al., 2010. Water Sources, Fourth Edition.

Greenwood, N.N. and Earnshaw, A., 2012. Chemistry of the Elements. Elsevier.

Reece, Jane B., 2013. Campbell Biology (10 ed.). Pearson. p. 48. ISBN 9780321775658.

Sweeney, D. and Williamson, B., 2006. Biology: Exploring Life: Laboratory Manual. Pearson Education, Incorporated.

Action–Liquid, C. and Water, F., 2013. Surface–JRank Articles. Science. jrank. org. Retrieved.

Isaacs, E.D., Shukla, A., Platzman, P.M., Hamann, D.R., Barbiellini, B. and Tulk, C.A., 2000. Compton scattering evidence for covalency of the hydrogen bond in ice. Journal of Physics and Chemistry of Solids, 61(3), pp.403-406.

Kenneth M. Vigil, P.E. 2003. Clean Water An Introduction to Water Quality and Water Pollution Control. Oregon State University Press Corvallis.

World Health Organization, 2004. Guidelines for drinking-water quality (Vol. 1). World Health Organization.

Radziemski, L.J. and Loree, T.R., 1981. Laser-induced breakdown spectroscopy: time-resolved spectrochemical applications. Plasma Chemistry and Plasma Processing, 1(3), pp.281-293.

Amoruso, S., Bruzzese, R., Spinelli, N. and Velotta, R., 1999. Characterization of laser-ablation plasmas. Journal of Physics B: Atomic, Molecular and Optical Physics, 32(14), p.R131.

Russo, R.E., Mao, X., Liu, H., Gonzalez, J. and Mao, S.S., 2002. Laser ablation in analytical chemistry—a review. Talanta, 57(3), pp.425-451.

Griem, H.R., 2005. Principles of plasma spectroscopy (Vol. 2). Cambridge University Press.

Dolgaev, S.I., Simakin, A.V., Voronov, V.V., Shafeev, G.A. and Bozon-Verduraz, F., 2002. Nanoparticles produced by laser ablation of solids in liquid environment. Applied surface science, 186(1-4), pp.546-551.

Richard W. Solarz; Jeffrey A. Paisner, 1986. Laser Spectroscopy and its Applications. CRC Press. *pp. 623–*. ISBN 978-0-8247-7525-4.

Schultz, I., 2014. Practical applications of laser absorption spectroscopy for aeroengine testing (Doctoral dissertation, Stanford University).

Peter Larkin, 2011. Infrared and Raman Spectroscopy Principles and Spectral Interpretation, Elsevier.

Tu, A.T., 1982. Raman spectroscopy in biology. Principles and Applications,1.

Edwards HG., 2005. Modern Raman spectroscopy-a practical approach. Ewen Smith and Geoffrey Dent. John Wiley and Sons Ltd, Chichester, Pp. 210. ISBN 0 471 49668 5 (cloth, hb); 0 471 49794 0 (pbk).

Ferraro, J.R., 2003. Introductory raman spectroscopy. Elsevier.

W. Demtroder, 2008, laser spectroscopy, Fourth edition, Springer-VerlagBerlin Heidelberg, ISBN 978-3-540-73415-4.

Adar, F., 1988. Developments of the Raman microprobe-Instrumentation and applications. Microchemical journal, 38(1), pp.50-79.

Marek Procházka, 2016. Surface-Enhanced Raman Spectroscopy Bioanalytical, Biomolecular and MedicalApplications, Institute of Physics, Charles University inPrague, Prague 2, Czech Republic.

Clark, J., 2000. The fingerprint region of an infra-red spectrum.

Friesen, M., Junker, M., Zumbusch, A. and Schnöckel, H., 1999. Raman-spectroscopy of oligomeric SiO species isolated in solid methane. The Journal of chemical physics, 111(17), pp.7881-7887.

Urabe, H., Tominaga, Y. and Kubota, K., 1983. Experimental evidence of collective vibrations in DNA double helix (Raman spectroscopy). The Journal of Chemical Physics, 78(10), pp.5937-5939.

Schütz, M., Müller, C.I., Salehi, M., Lambert, C. and Schlücker, S., 2011. Design and synthesis of Raman reporter molecules for tissue imaging by immuno-SERS microscopy. Journal of biophotonics, 4(6), pp.453-463.

Jain, R., Calderon, D., Kierski, P.R., Schurr, M.J., Czuprynski, C.J., Murphy, C.J., McAnulty, J.F. and Abbott, N.L., 2014. Raman spectroscopy enables noninvasive biochemical characterization and identification of the stage of healing of a wound. Analytical chemistry, 86(8), pp.3764-3772.

Butler, H.J., Ashton, L., Bird, B., Cinque, G., Curtis, K., Dorney, J., Esmonde-White, K., Fullwood, N.J., Gardner, B., Martin-Hirsch, P.L. and Walsh, M.J., 2016. Using Raman spectroscopy to characterize biological materials. Nature protocols, 11(4), p.664.

Vandenabeele, P., Edwards, H.G. and Moens, L., 2007. A decade of Raman spectroscopy in art and archaeology. Chemical reviews, 107(3), pp.675-686.

Vogel, B., 2008. Raman spectroscopy portends well for standoff explosives detection. IHS Jane's.

Hardy, T.D.; Murowinski, R.G.; Deen, M.J., 1998. Charge transfer efficiency in proton damaged CCD's. IEEE Trans. Nucl. Sci. 45, 154–163.

Hardy, T.D.; Deen, M.J.; Murowinski, R.G., 1999. Effects of radiation damage on scientific charge coupled devices. Adv. Imaging Electron Phys. 106, 1–96.

Appendix

International Journal of Trend in Scientific Research and Development (IJTSRD)
Volume: 3 | Issue: 3 | Mar-Apr 2019 Available Online: www.ijtsrd.com e-ISSN: 2456 - 6470

The Ability of Raman Spectroscopy to Detect Surface Water Pollution in Northern Sudan

Sufyan Sharafedin Mohammed[1], A. M. Awadelgied[2], Sohad saad El Wakeel[3], Ahmed Abubaker Mohamed[3]

[1]Ph.D Student, [2]Professor, [3]Assistant Professor
[2]Karary University, Omdurman, Sudan, North Africa
[1,3]Sudan University of Science and Technology, Institute of laser. Sudan, North Africa

How to cite this paper: Sufyan Sharafedin Mohammed | A. M. Awadelgied | Sohad saad El Wakeel | Ahmed Abubaker Mohamed "The Ability of Raman Spectroscopy to Detect Surface Water Pollution in Northern Sudan" Published in International Journal of Trend in Scientific Research and Development (ijtsrd), ISSN: 2456-6470, Volume-3 | Issue-3, April 2019, pp.1805-1811, URL: https://www.ijtsrd.com/papers/ijtsrd22906.pdf

IJTSRD22906

ABSTRACT

Water pollution is a complex problem for people in Sudan, especially in the northern state. Human activities such as Gold exploration, use of fertilizers in agriculture and industrial activities are, more or less directly, responsible for increasing pollution in running waters. This study aims to detecting the contaminants present in surface water in Northern Sudan.

Five samples of water lines from different drinking water treatment plant were collected. the samples were analyzed by Horiba Lab RAM 3D Raman spectrometer. The results showed that the samples beside the water contain toxic and dangerous substances that may lead to dangerous diseases, in different quantities, such as: cyanide, nitrate, Uranium oxide and phenol.

KEYWORDS: Raman spectroscopy; Surface water pollution; dangerous diseases; water treatment plant; Northern Sudan

International Journal of Fluid Mechanics & Thermal Sciences
2019; 5(1): 28-35
http://www.sciencepublishinggroup.com/j/ijfmts
doi: 10.11648/j.ijfmts.20190501.13
ISSN: 2469-8105 (Print); ISSN: 2469-8113 (Online)

Characterization of Surface Water Components in Northern Sudan Using Raman Spectroscopy

Sufyan Sharafedin Mohammed[1], Abdelmoneim Mohammed Awadelgied[2], Sohad Saad El Wakeel[1], Ahmed Abubaker Mohamed[1]

[1]Department of Physics, Sudan University of Science and Technology, Institute of Laser, Khartoum, Sudan

[2]Department of Engineering, Karary University, Khartoum, Sudan

Email address:

sufyansharaf@gmail.com (S. S. Mohammed), sohaddiga@sustech.edu (S. S. El Wakeel), Ahmedabubaker5555@gmail.com (A. A. Mohamed), Moneim60@yahoo.com (A. M. Awadelgied)

To cite this article:

Sufyan Sharafedin Mohammed, Abdelmoneim Mohammed Awadelgied, Sohad Saad El Wakeel, Ahmed Abubaker Mohamed. Characterization of Surface Water Components in Northern Sudan Using Raman Spectroscopy. *International Journal of Fluid Mechanics & Thermal Sciences*. Vol. 5, No. 1, 2019, pp. 28-35. doi: 10.11648/j.ijfmts.20190501.13

Received: March 31, 2019; **Accepted**: May 5, 2019; **Published**: May 31, 2019

Abstract: Most population in northern Sudan are supplied by surface water sources directly from the Nile for drinking and irrigation purposes. As noted, most of them suffer from chronic diseases such as cancer and kidney failure. Water is expected to be a major and direct cause of these diseases, so the aim of this study is to identify the components of surface water in northern Sudan using Raman spectroscopy. Surface water Samples were collected from the Nile in different regions. The samples were analyzed at room temperature using Raman spectrometer model Horiba Lab RAM HR D3. The results showed that the samples contain different materials, beside the water, with different amounts; like: aromatic molecules, ester, salts, amides, phenol, alkynes and acids. From the results we have found that the water contains many toxic compounds such as cyanide, nitrate and phenol, which is one of the most important causes of cancer and renal failure. As well as can cause oxidize the iron atoms in hemoglobin from ferrous iron (II) to ferric iron (III), rendering it unable to carry oxygen. This process can lead to generalized lack of oxygen in organ tissue and a dangerous condition called methemoglobinemia.

Keywords: Raman Spectroscopy, Surface Water Characterization, Surface Water in Northern Sudan